Rzhanov Institute of Semiconductor Physics, Novosibirsk, Russia

Diamond-Graphite-Diamond Heterostructures Produced by Implantation and HPHT Annealing for Lift-off Transfer and New Devices

V.P. Popov, ***V.A. Antonov, S.N. Podlesny, M.A. Ilnitskii, A.K.Gutakovskii,***

I.N. Kupriyanov, Yu.N. Pal'yanov

Tomsk 2017

Sobolev Institute of Geology and Mineralogy, Novosibirsk, Russia

Maximal breakdown voltage and mobility vs. doping

$$E_{c,\,dia} = 10^7\ V{\cdot}cm^{-1}$$

$$V_B \approx \frac{\varepsilon_r E_c^2}{2qN_d}$$

E_c = electric breakdown field

$N_d = 10^{17}\ cm^{-3}$

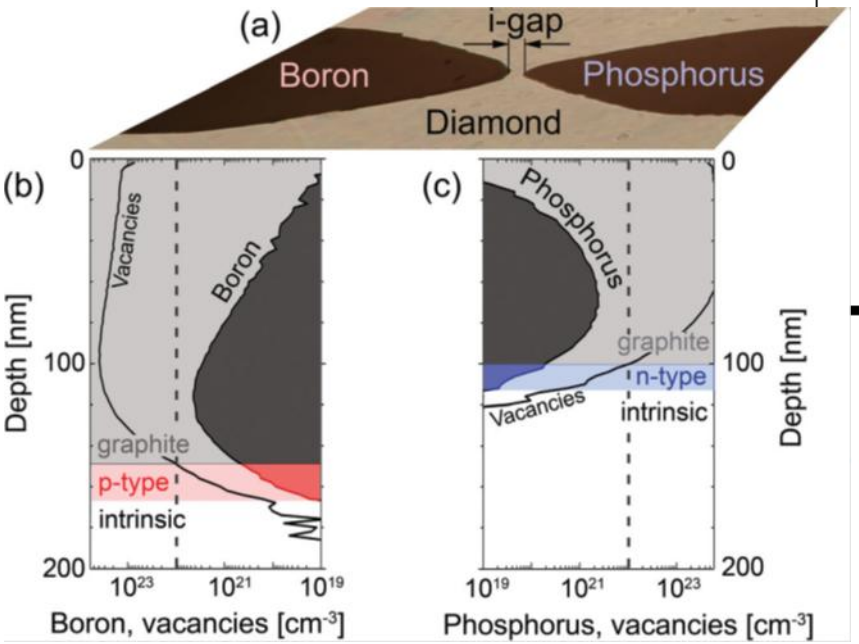

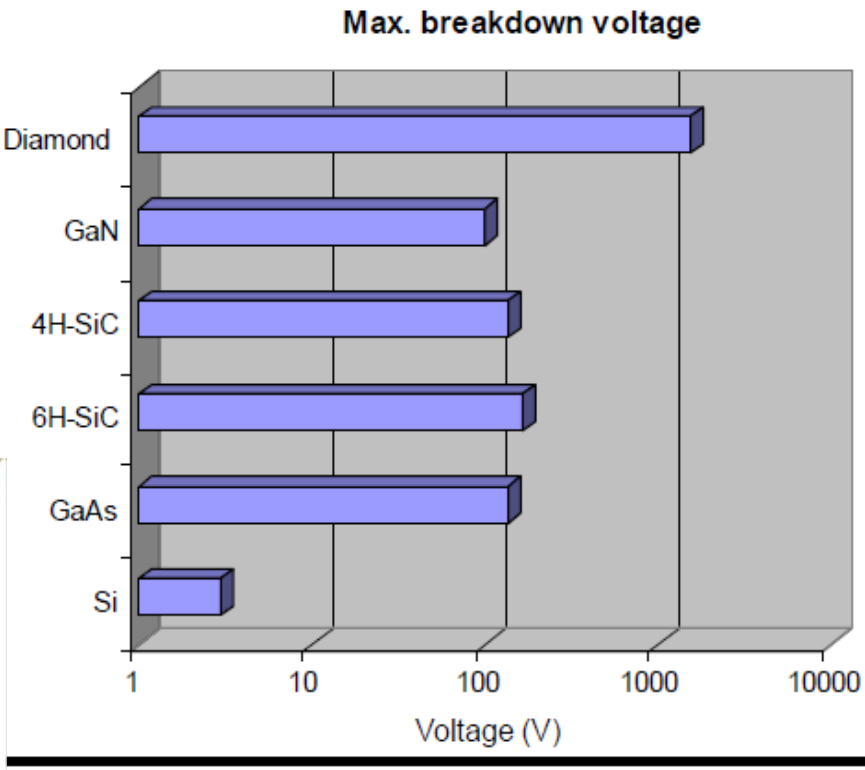

diamond is 10 times better than all others

51, 14-21 (1999).

A. Lohrmann,1 S. Pezzagna,1 I. Dobrinets et al. Appl.Phys.Lett. 99, 251106 (2011)

Band alignment and resistivity of diamond and graphite

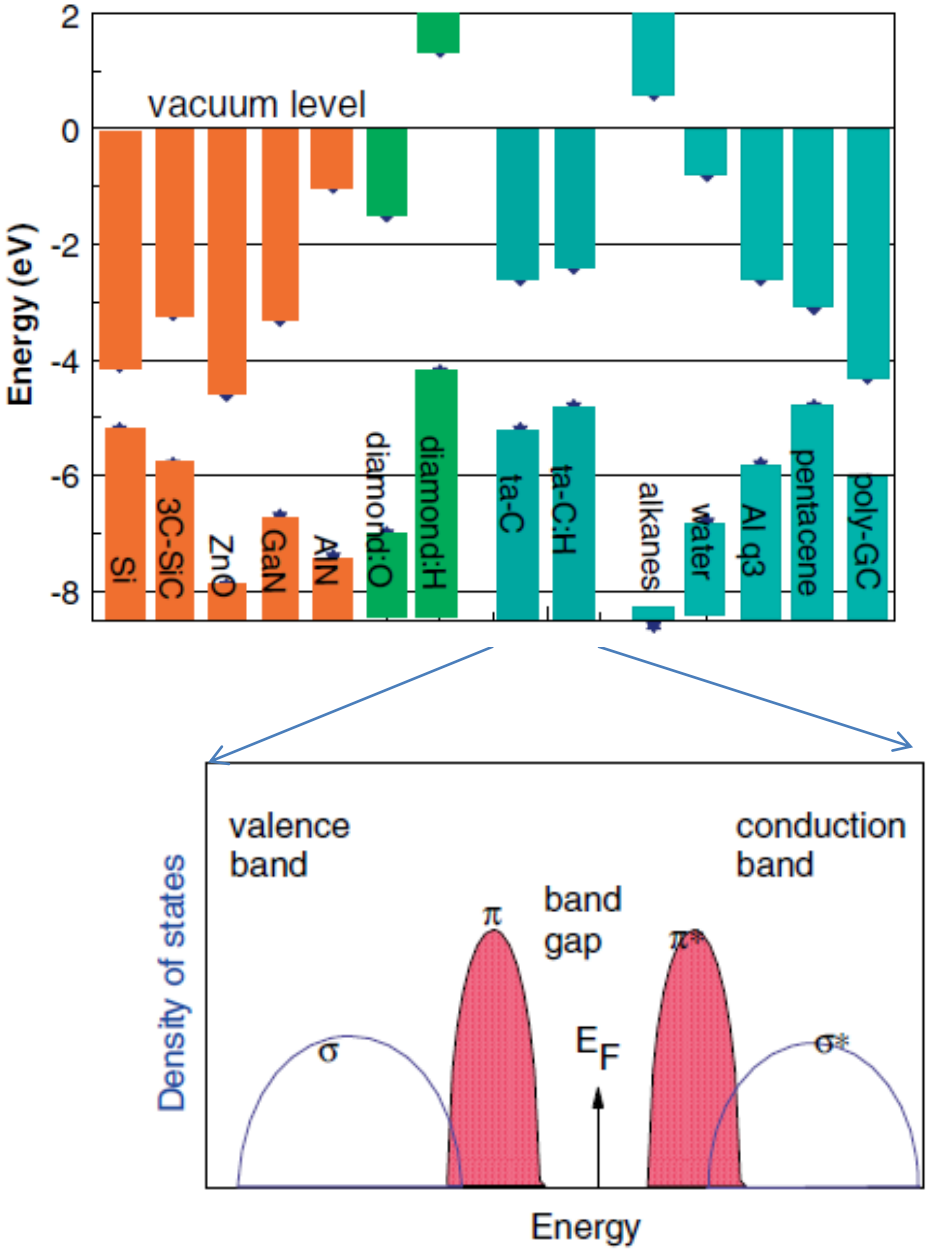

Material	Resistivity (Ω·cm)
Diamond	$10^{13} \div 10^{15}$
Graphite	$10^{-5} \div 5 \cdot 10^{-3}$
Laser-modified material	3.6÷3.9
Partially graphitized diamond [1]: after ion bombardment after following annealing	 10^{2} 10^{-3}

[1] A. Reznik et al., Phys. Rev. B 56 (1997) 7930.

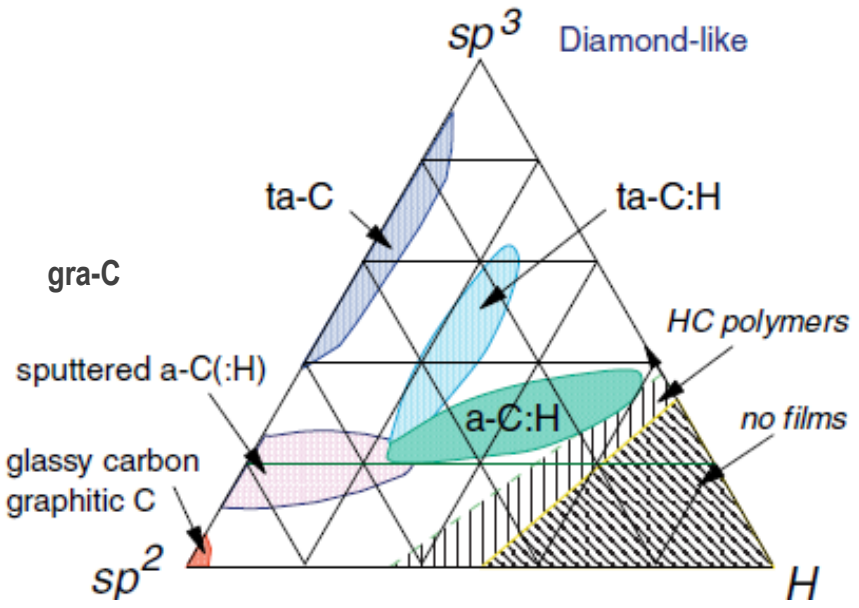

J. Robertson, phys. stat. sol. (a) 205, No. 9 (2008)

Motivation

Normally-On MESFET: I_{on}= 1300mA/mm

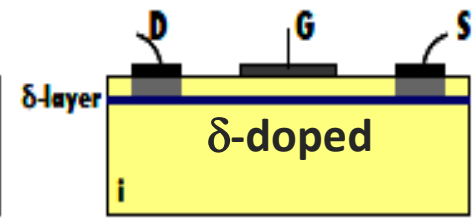

δ-FET

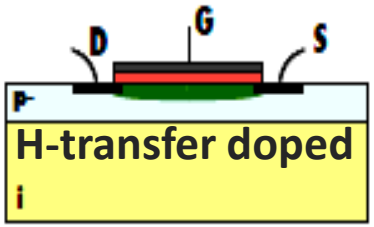

MOSFET

Hirama K.*et al*.
JJAP 51 (2012) 090112

Normally-Off MISFET & MESFET: 10mA/mm

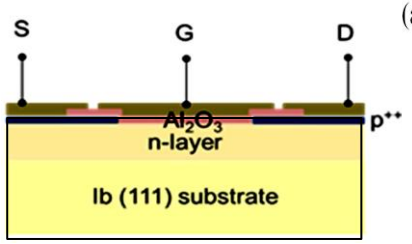

Inversion channel MISFET

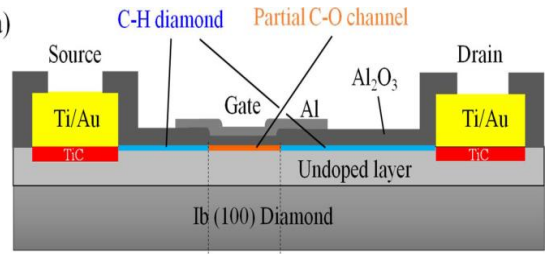

Partial C-O channel MESFET

Y Kitabayashi et al.
IEEE EDL, 38 (2017) 363

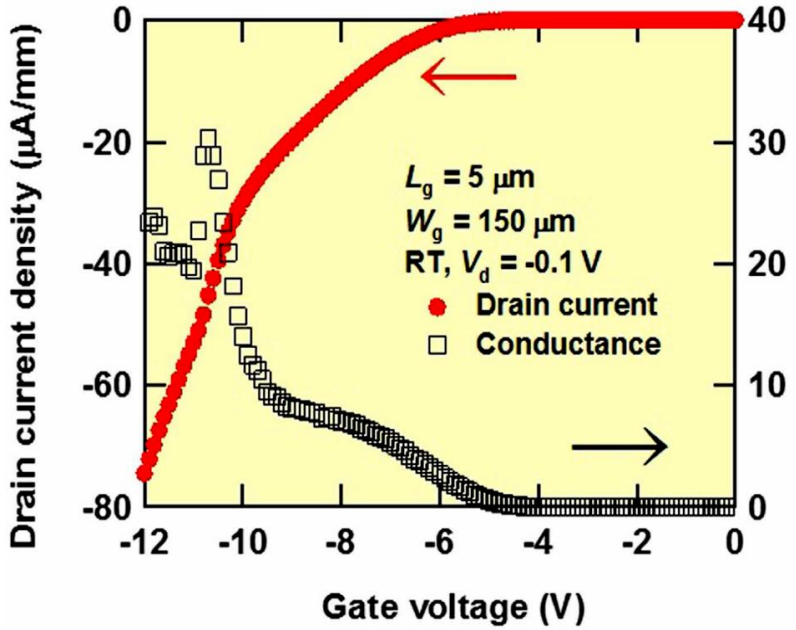

T.Matsumoto *et al*. *Sci. Rep.* ***6*** *(2016) 31585*

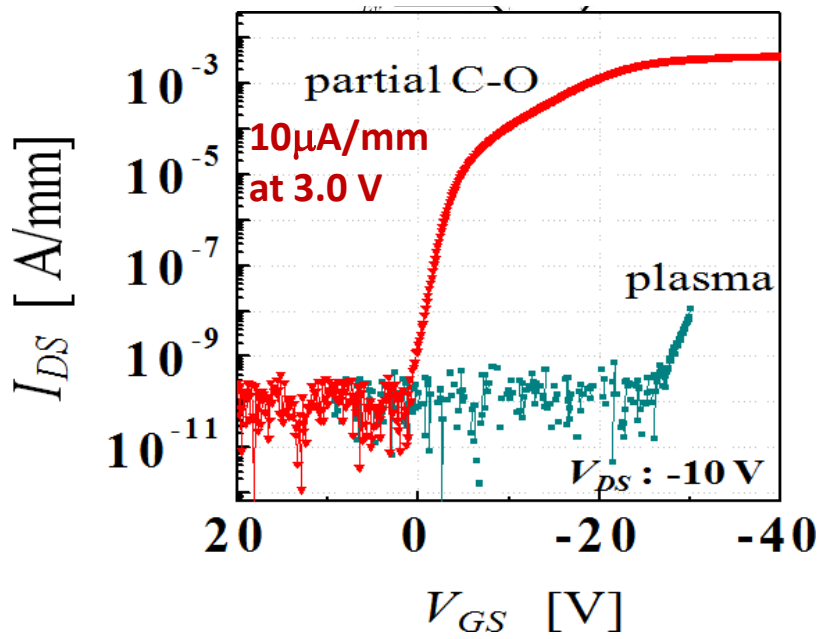

Normally-Off MOSFET: low current at $V_{GS} \leq 3$ V !

Diamond as a coolest material for Quantum Information Processing

Status of diamond relative to DiVincenzo criteria for Quantum Information Processing (QIP):

T_D = 1860 K

	Criteria	Low temp	Room temp
1	Well-defined qubits	✓	✓
2	Initialization to a pure state	✓	✓
3	Universal set of quantum gates	✓	✓
4	Qubit-specific measurement	✓	Progressing well
5	Long coherence times	✓	✓
6	Interconvert stationary and flying qubits	Progressing well	Maybe
7	Transmit flying qubits to distant locations	Progressing well	Progressing well

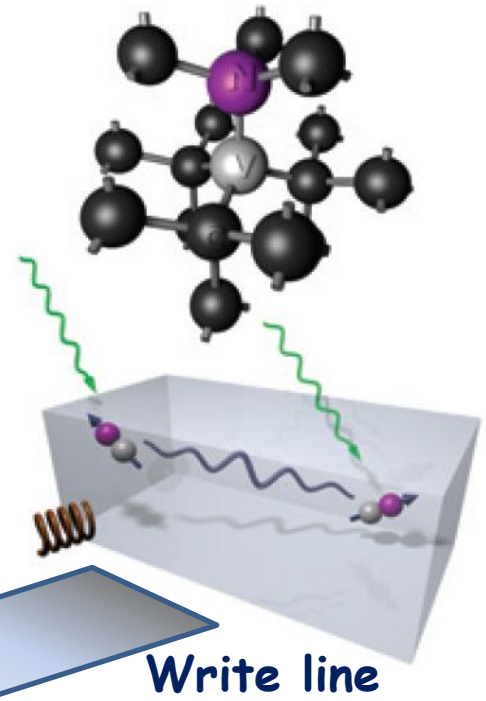

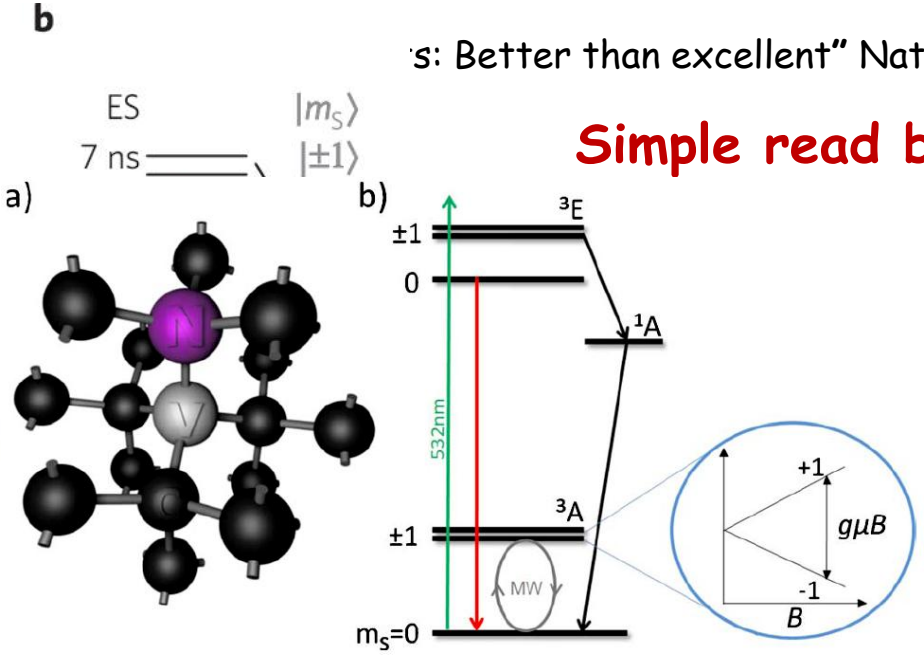

's: Better than excellent" Nature Mat. **9**, 468–469 (2010)

Simple read by CCD matrix…

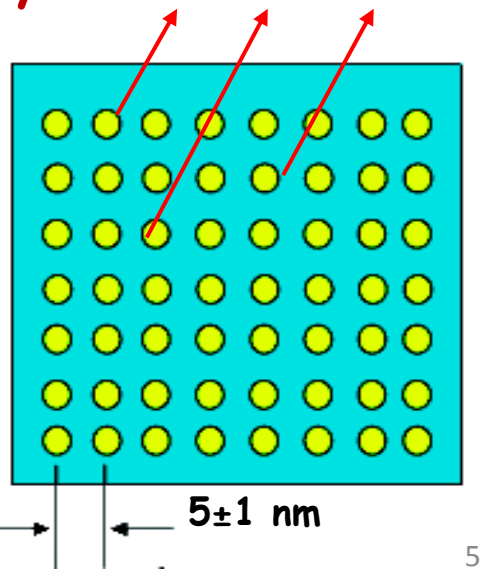

Joerg Wrachtrup "Defect center room-temperature quantum processors", *Proc. Natl. Acad. Sci. USA* **107**, 9479 (2010).

…but it is still not implemented !

Outlook

1. Motivation for Diamond Electronics
2. Diamond-Graphite-Diamond by II & Lift-off Process
3. Diamond Junction & Field Effect Transistors (J- & FET's)
4. Sensing by Membranes & NV Defects in Nanostructures
5. Conclusion

Forms and sizes of type Ib, IIb, IIa HPHT diamond samples

HPHT growth in Fe-Ni-C liquid from the seed

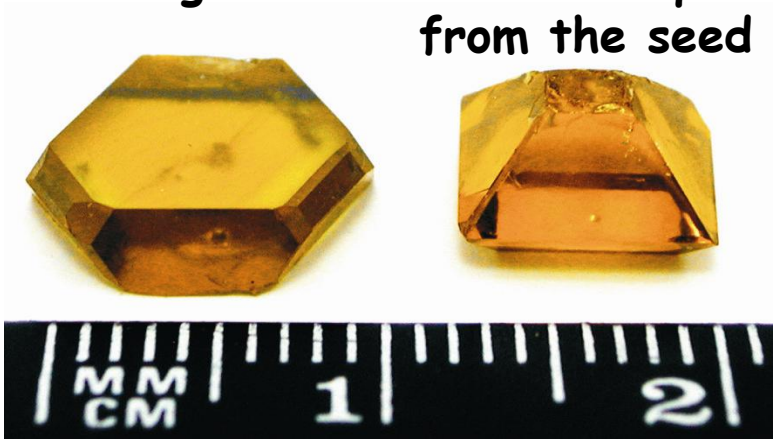

{111} Ib type crystal (left) and {100} (right) with the area up to 40 mm^2 was grown using (111) seed orientation for 3-4 carat size

{100} IIa type crystal with the area up to 30 mm^2 was grown using (111) seed orientation for 2-3 carat size

Laser cleavage and grinding by diamond nanocrystal slurry

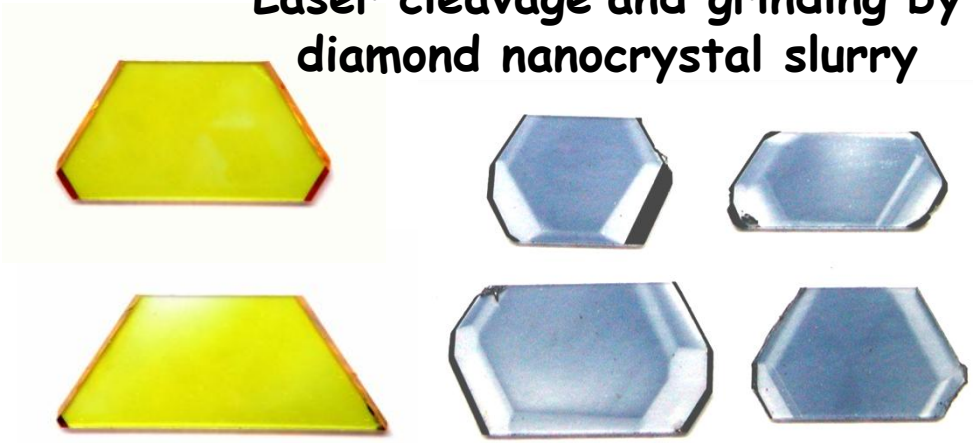

200-400 μm plates of {111} plates with the area up to 25 mm^2 were produced by laser pointing with subsequent cleavage along the plane of the spikes, grinding & polishing or CVD overgrowth.

Doped by B or N (1.0-100 ppm) and undoped (<0.1 ppb) samples were used.

How to produce 3-4 order of magnitude thinner slices ???

Using beam spliting:

See our Poster no.26

Proton and Molecular Ion Range (SRIM) & Peak Position (SIMS)

How cut diamond on the slices by ion injector?

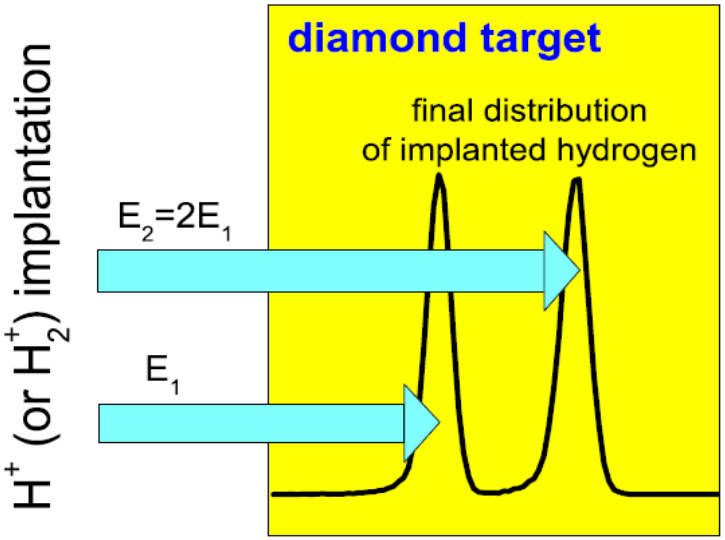

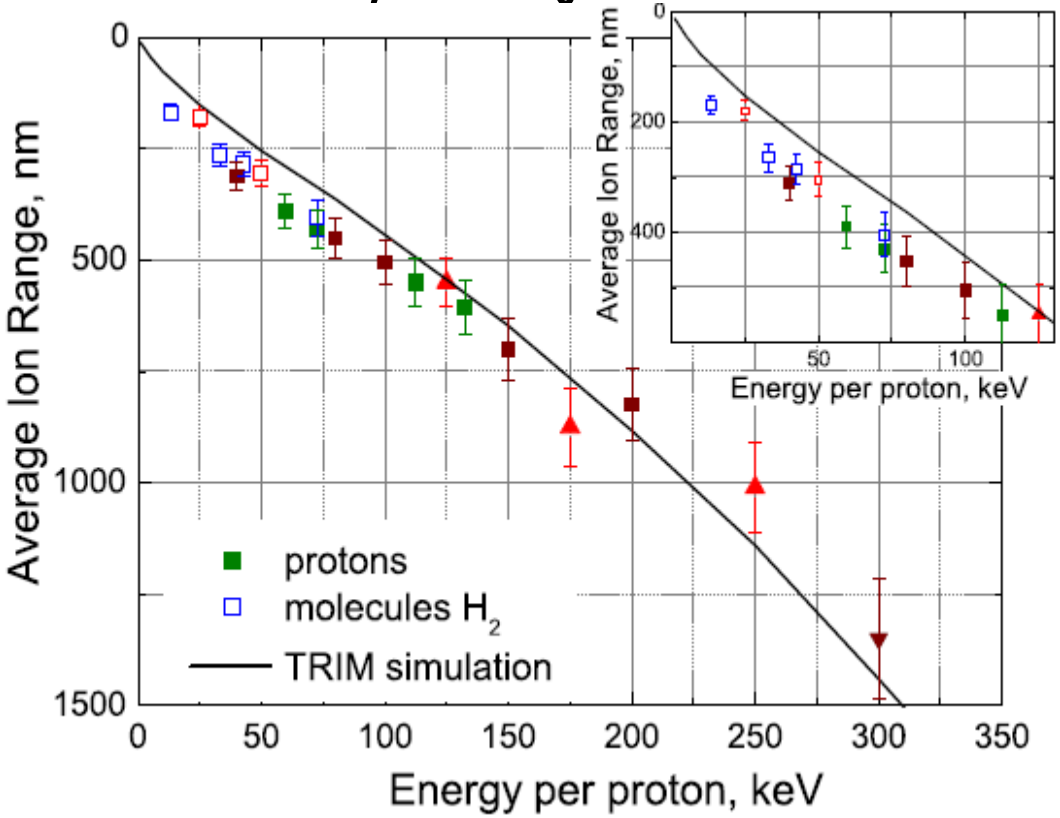

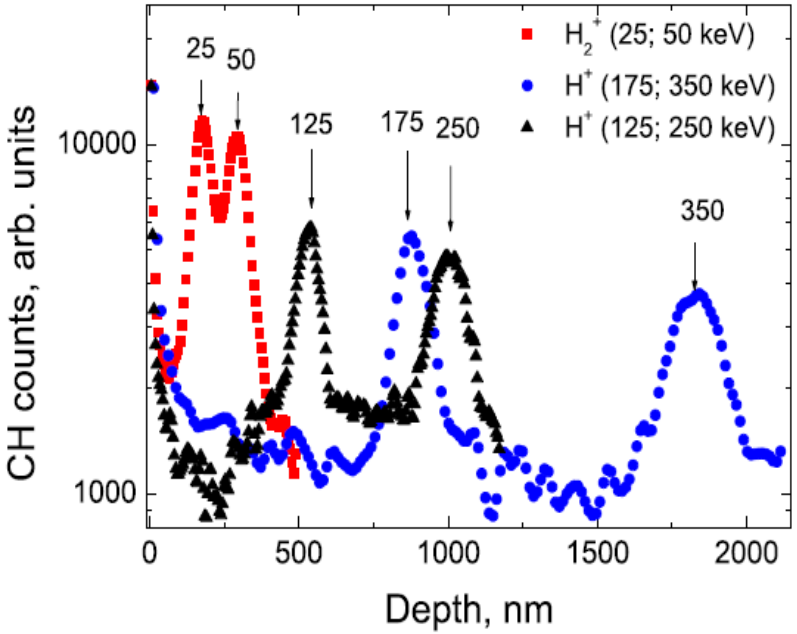

Is injection implantation at. V >50 kV reasonable for multiple cut?

2:1 Relation in the flux between protons and molecular ions is needed.

ESR source allows making this!

V.P. Popov et al. NIM B 406 (2017) 634–637

Defect profiles & graphitization after H⁺II + HPHT

Graphitization : $Ncrit = 10^{22} Vac/cm^3$

Hydrogen mol. 60 keV

$Dcrit = 5*10^{16} H_2^+ / cm^3$

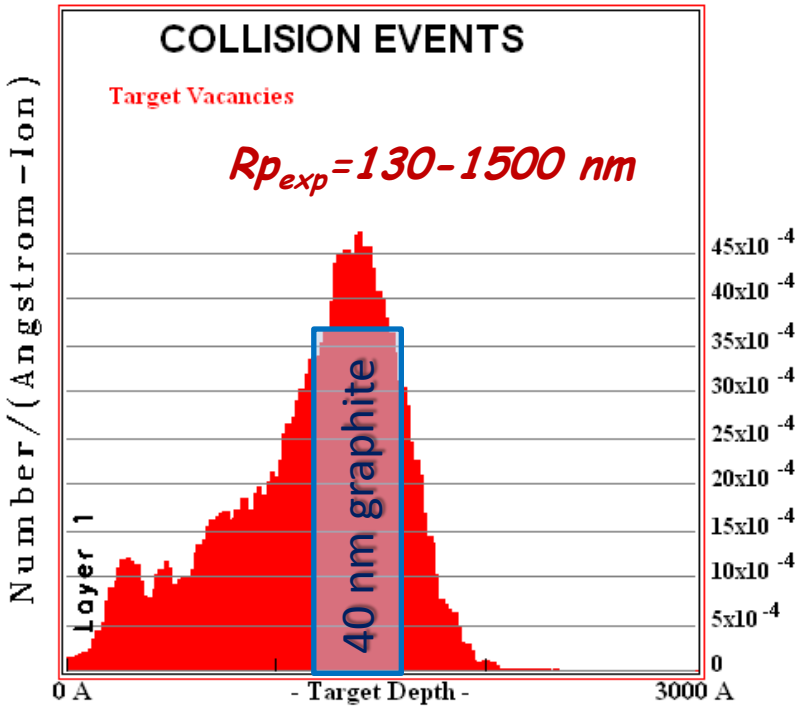

Nitrogen 130 keV

$Dcrit = 5*10^{14} N^+ / cm^3$

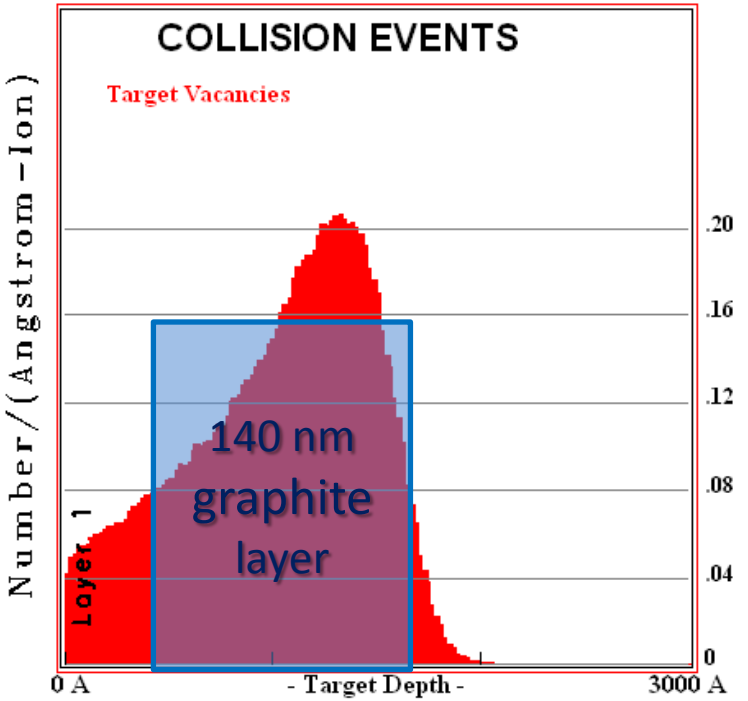

Swelling: $T^N gr > T^N am > T^N crit$ is due to 10-40% lower density in innner layer.

The estimation of internal pressure using diamond mechanical properties

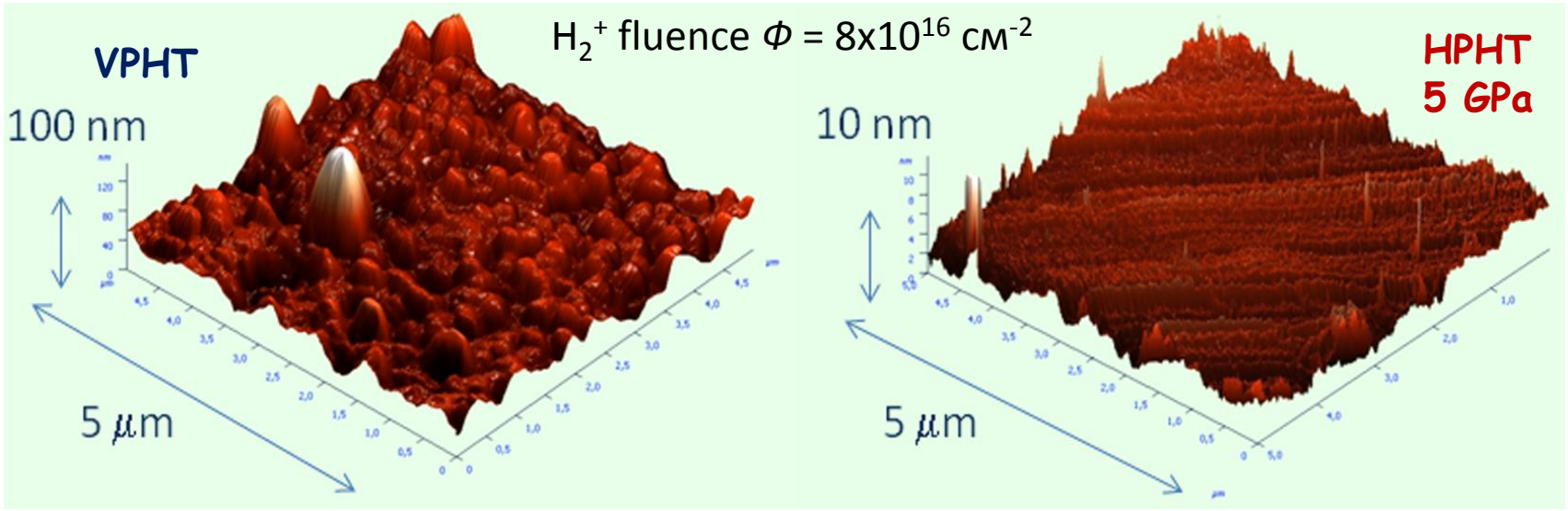

The pressure p_0 in blister (radius R, thickness of cup layer h) as a function of the maximum deflection δ is [*]:

$$p = p_0 + \frac{16}{3}\frac{\bar{E}h^3}{\langle R\rangle^4}\delta \qquad [1]$$

p_0 is outer pressure. $\bar{E} = E/(1-\nu^2)$ is biaxial elastic modulus with plane-strain modulus. E = 175±5 GPa Young's modulus to [111] direction. Poisson ratio ν = 0.1 [**]:

For VPHT *with h = 0.25 μm, R = 0. 5 μm,* δ *= 0.03 μm:* ***p = 7.0 GPa,***

For HPHT *with h = 0.25 μm, R = 0.5 μm,* δ *= 0.006 μm:* ***p = 7.0 GPa***

Young's modulus to [0001] graphite is equal to E = 32.5 GPa and ν = 0.3 : **p = 1.6 GPa,**

** C. Coupeau et al. Appl. Phys. Lett. 103 (2013) 031908*

*** V.Blank, et al. Diam. and Relat. Mater. 8 (1999) 1531.*

TEM/HREM planar view: diamond & graphite layers after H_2^+II & HPHT

Very rare defect region

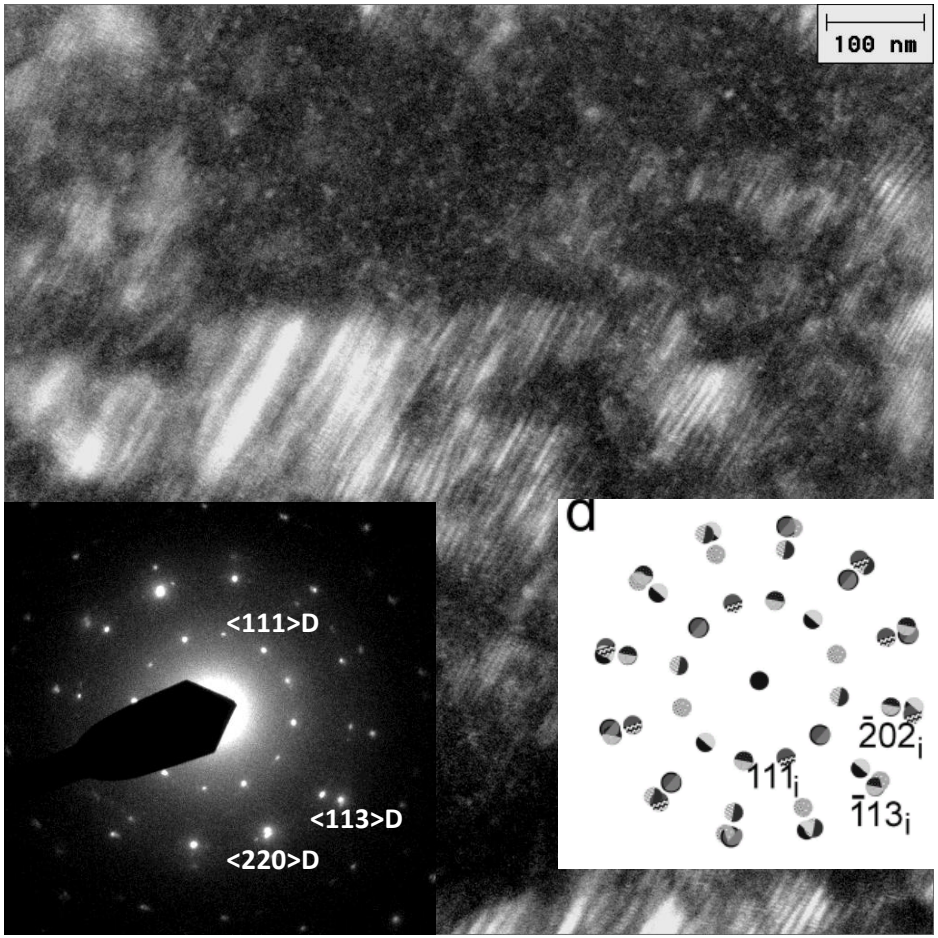

Dark field TEM of upper d-C layer (30÷50nm) with 12 diffraction spots due to nd-C twinning by 30° rotation along <111> direction leading to combination of cubic (d-C) and hexagonal (2H) diamond or grains

P.Nemeth et al. srep18381

Typical structure of glassy carbon layer

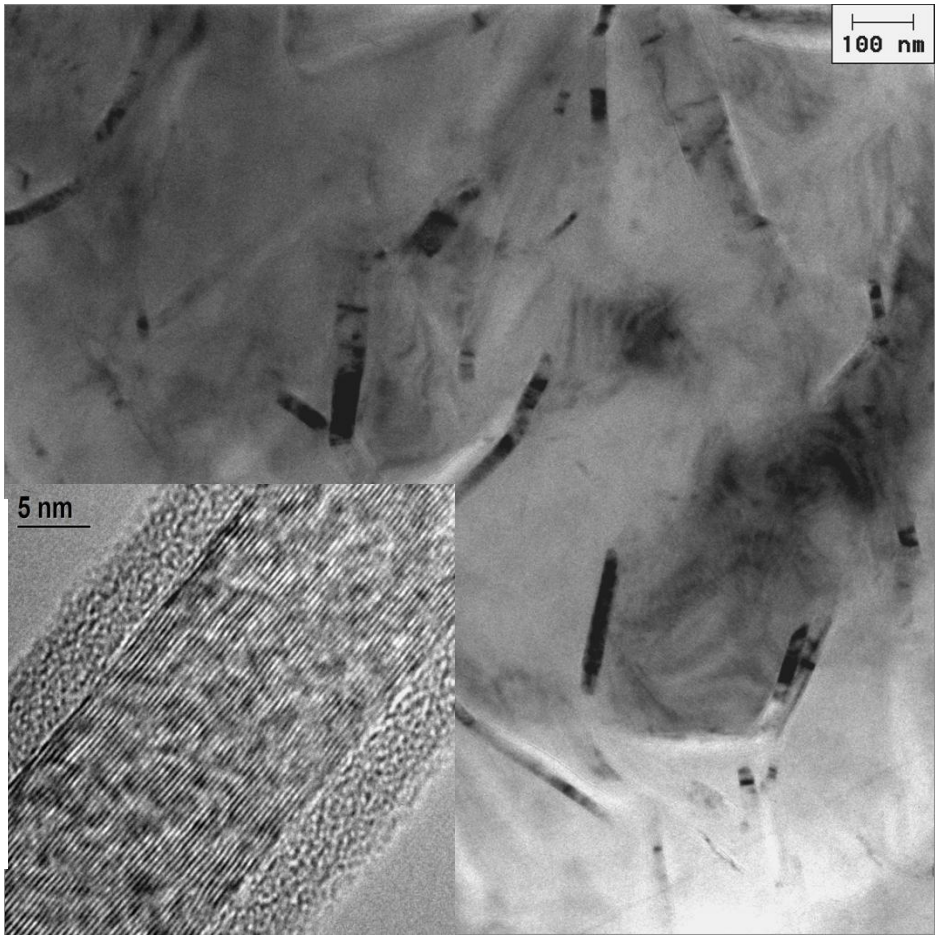

Glassy-C layer with thickness 100÷120 nm with vertical graphite nanolamellas inside with **interplanar spacing Δd = 0.35 nm**

First model for growth of graphite on (110) planes of diamond

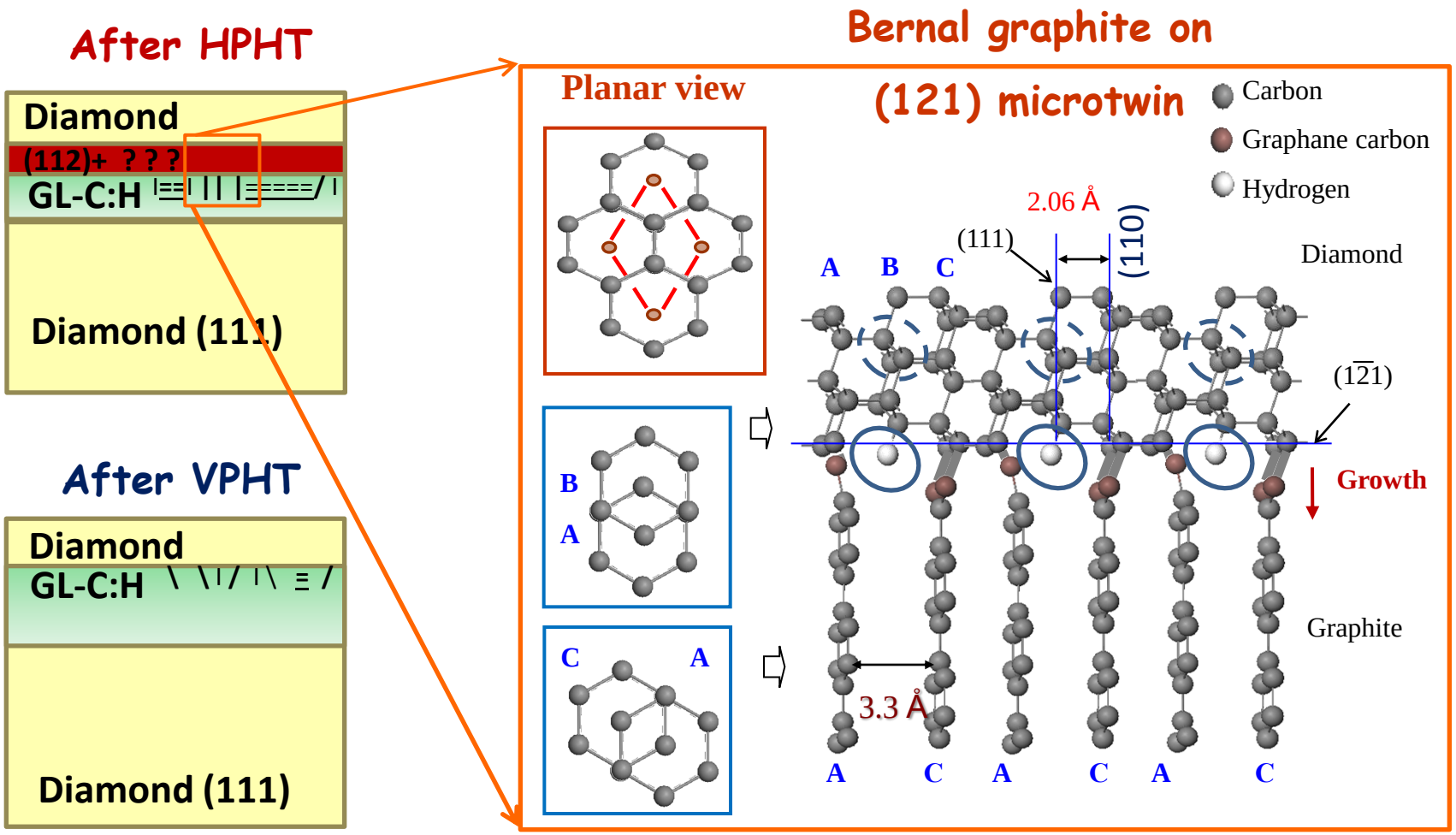

2:3 diamond growth model* – 3:2 graphite growth model for vertical planes

*W. R. L. Lambrecht et al., Nature **364**, (1993) 607-610

SAED, XTEM and FFT, HRTEM of HPHT annealed Ib (111) diamond

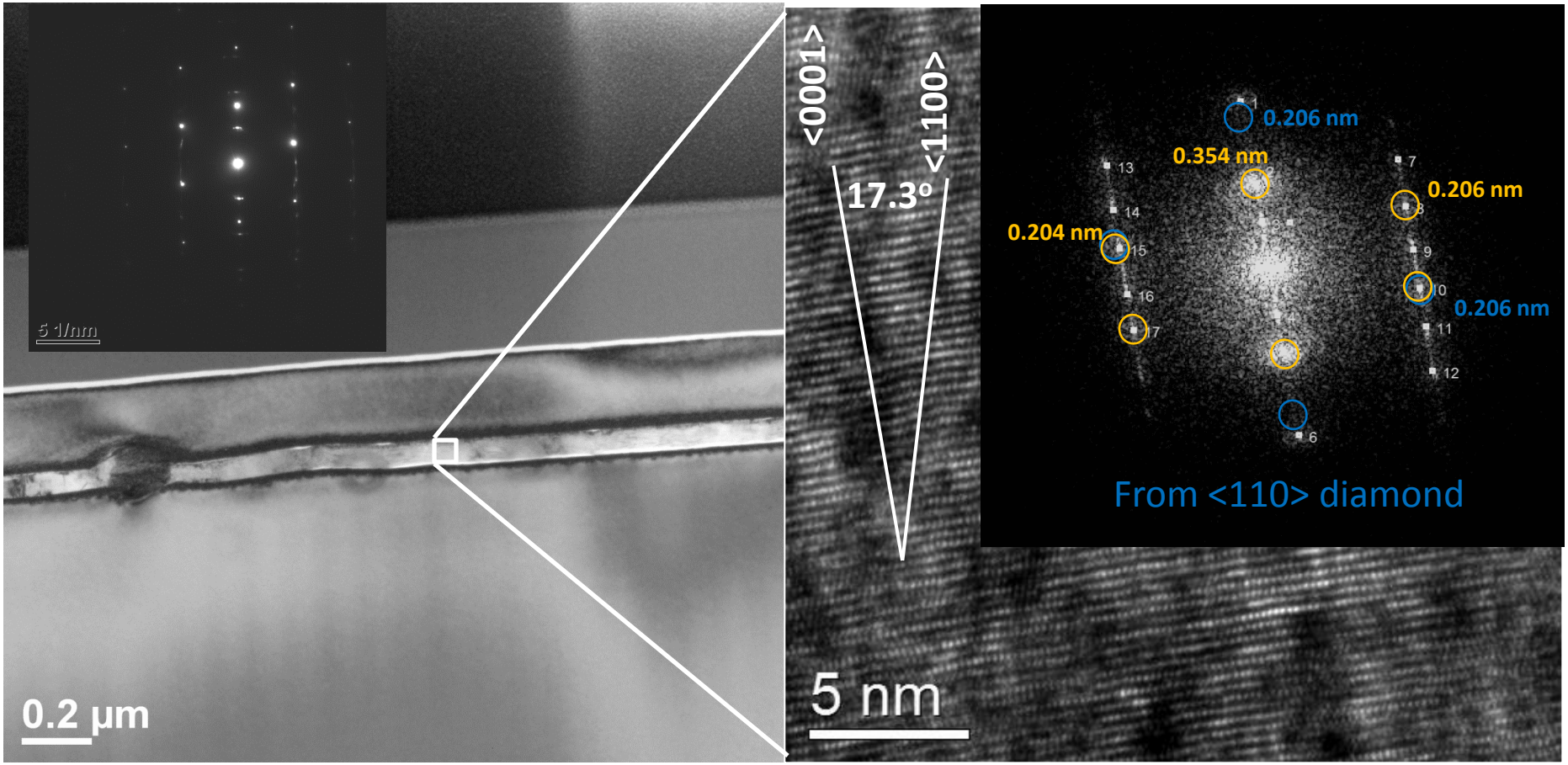

50 keV hydrogen molecule fluence $\Phi = 4 \times 10^{16}$ см$^{-2}$ after HPHT annealing at 1200°C 4 GPa 4 h

Graphite (nm): 0.335(111), 0.213(100),

Tetragonal distortion: d_{111} = 0.354 nm, d_{100} = 0.204 nm with 72.7° between <111> and <100> directions suggests mixed Bernal/rhombohedral graphene sheet package

Second model for growth of graphite on (111) planes of diamond

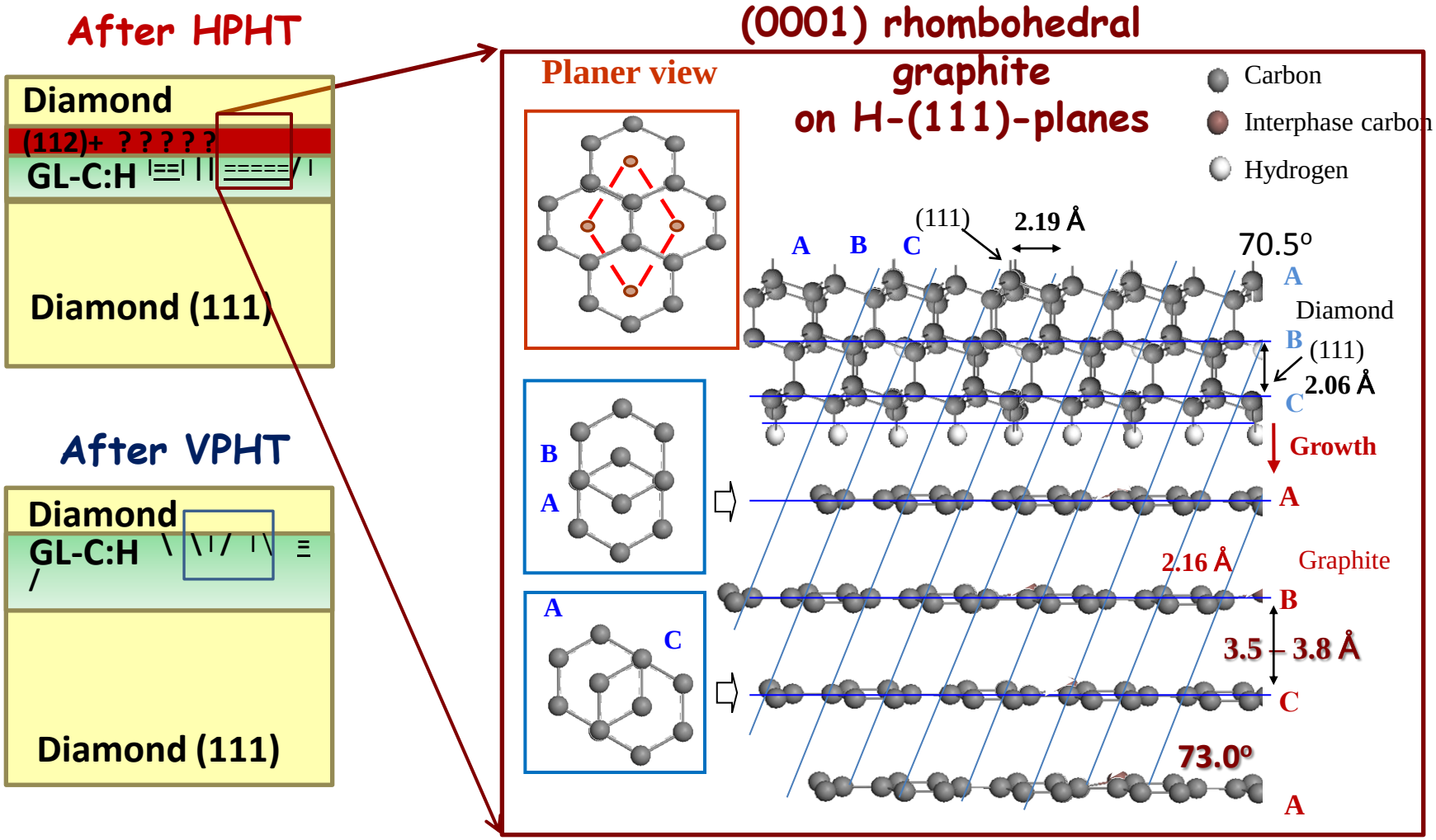

1/1 graphite growth model corresponds to the experimental angle ~17° and shows increased distances between carbon atoms and graphene planes

*V.P. Popov et al. AIP Conf. Proceed., 2012

HREM micrograph of buried layer and Raman spectra after H_2^+II & HPHT

Hydrogen molecules (H_2^+), 50 keV, (1÷13)x10^{17} cm^{-2} + Nitrogen (N^+), 120 keV, 3.5x10^{16} cm^{-2} (through Al-mask for contacts)
HPHT treat.: P=4÷8 GPa
T=1200÷1600°C, 4 h (BARS)
VPHT: P=10^{-3} Pa

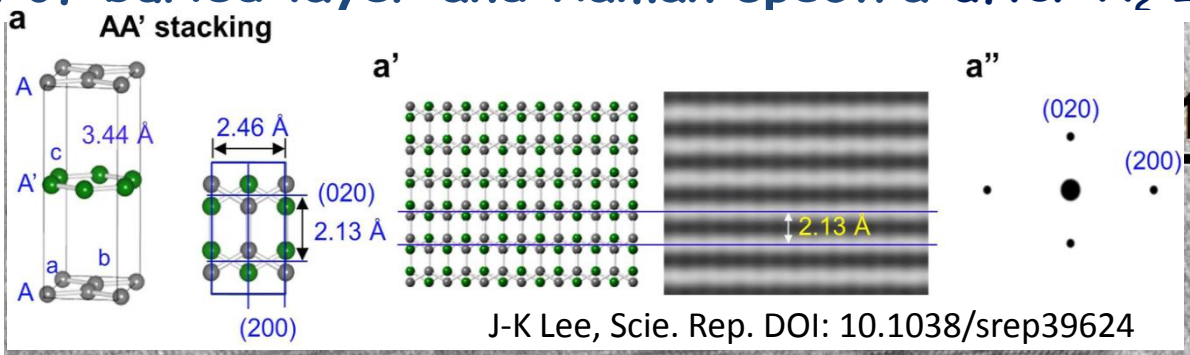

J-K Lee, Scie. Rep. DOI: 10.1038/srep39624

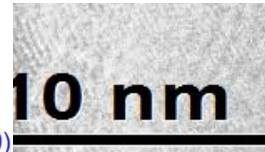

0.45 nm

Theoretic bigraphane interplanar distance* ~0.45÷0.50 nm

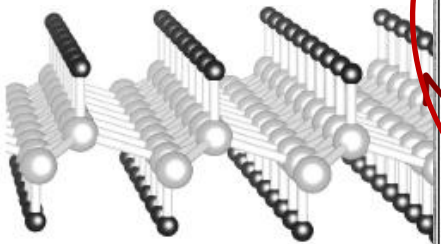

*J.K.Lee **Phys. Rev. B 83, 165423. 2011**

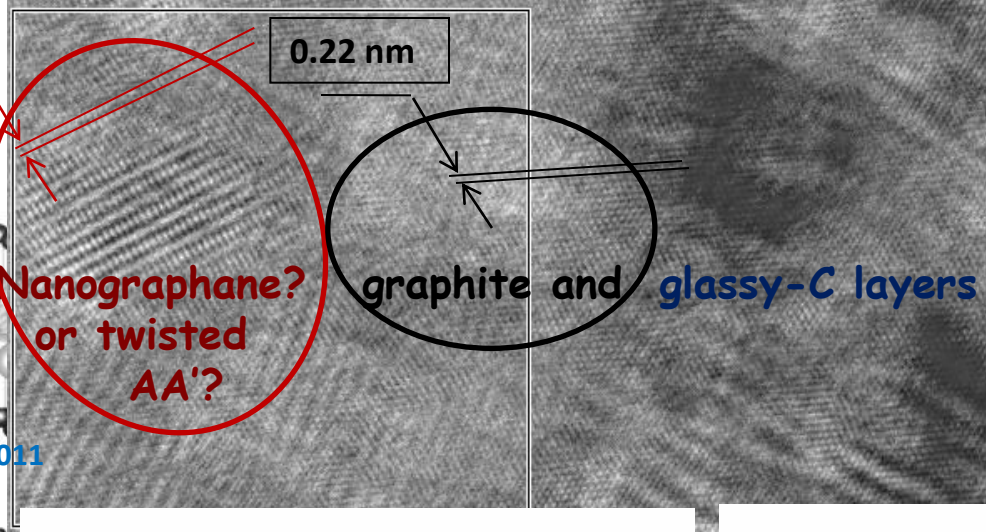

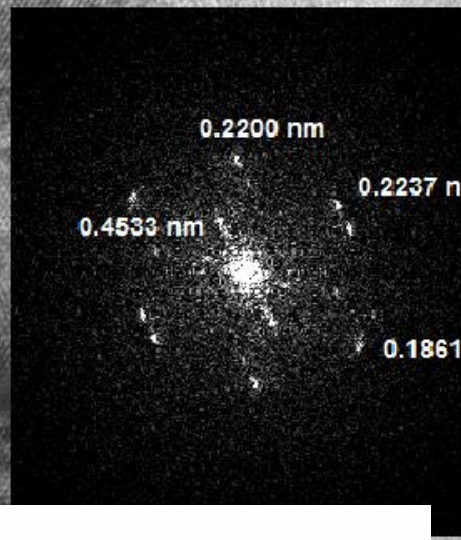

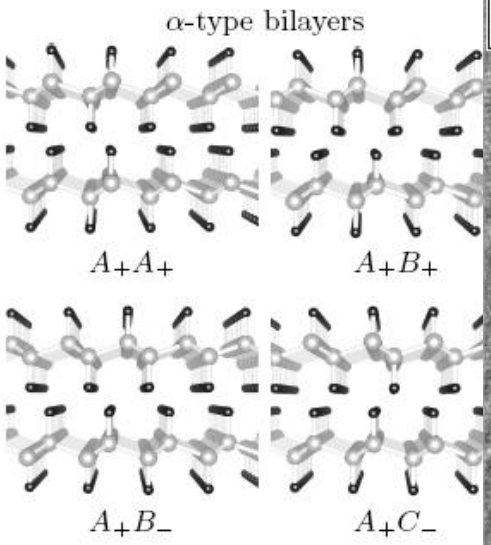

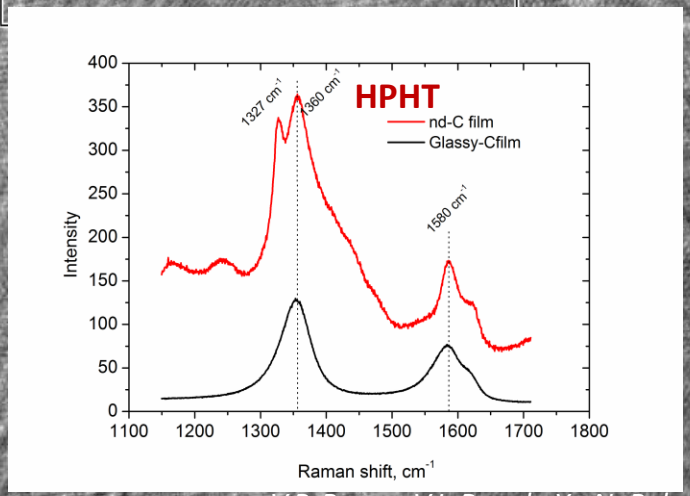

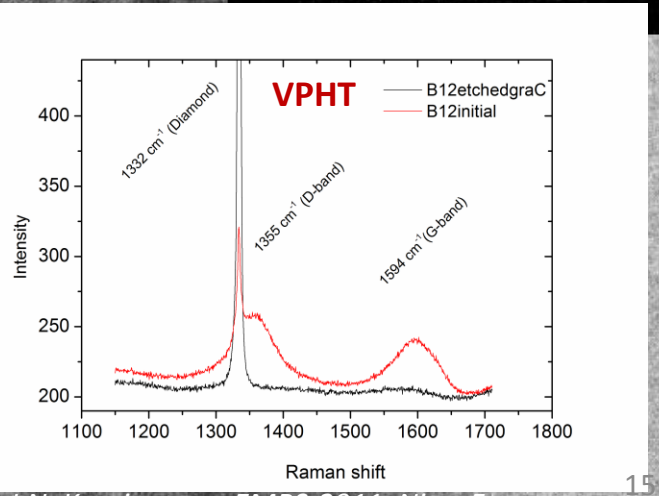

Applications for DGD-heterostructures

Amplifying of NV⁻centers PL in d-C Ib by E-field

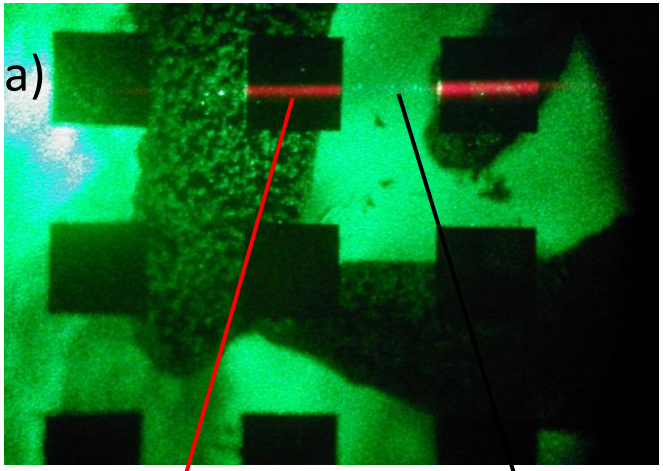

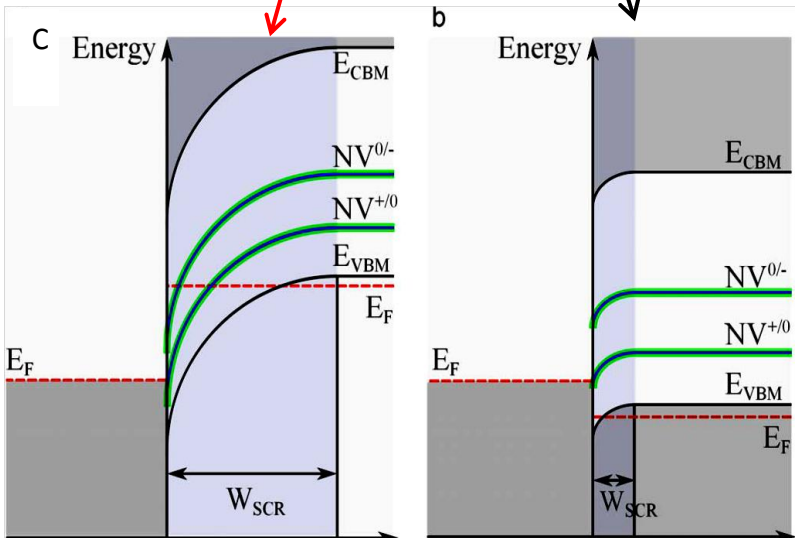

Graphite H-C Diamond Graphite H-C Diamond

CN-heterojunctions

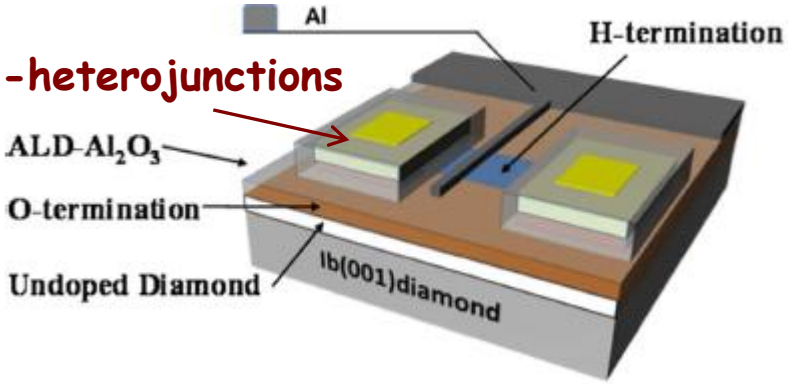

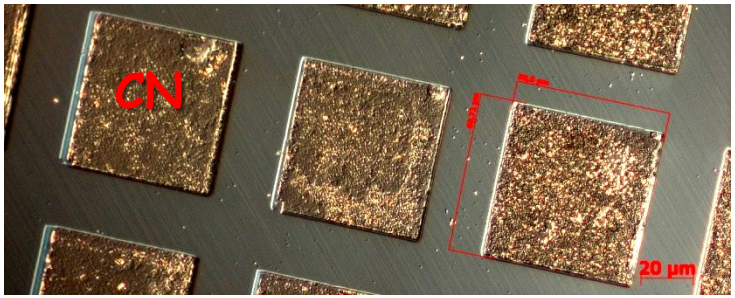

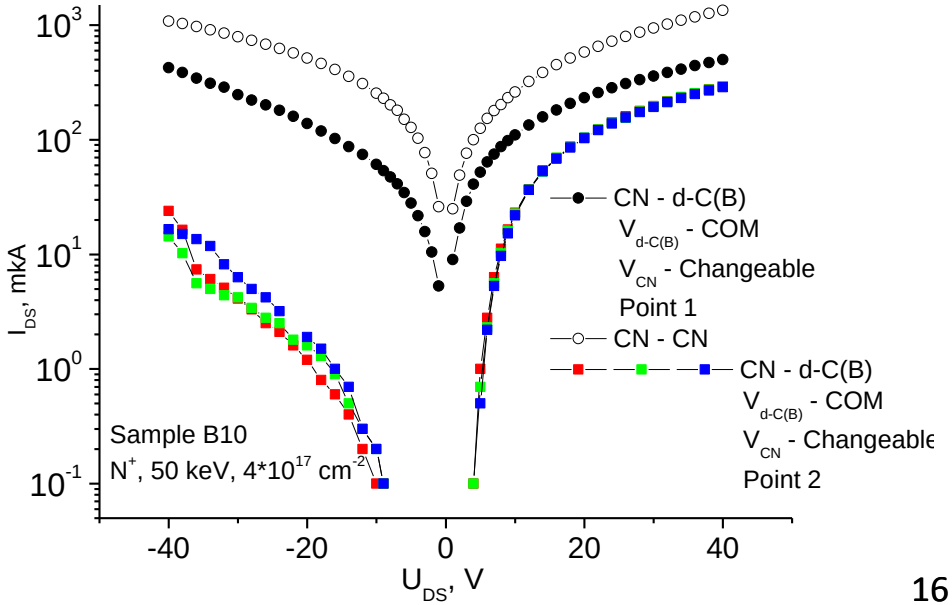

V.P. Popov *et al.* Int. J. Nanotechnol., 12, 226 , 2015.

Test structures for conductivity

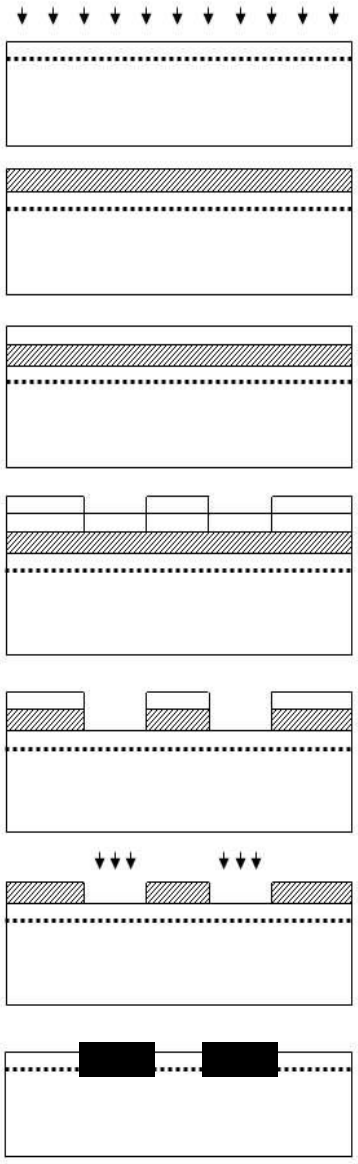

Hydrogen molecules (H_2^+), 50 keV, (1÷13)x10^{16} cm^{-2}

+ Nitrogen (N^+), 130 keV, 3.5x10^{16} cm^{-2} (through Al-mask for contacts)

VPHT treat.: P=10^{-3} Pa
HPHT treat.: P=4÷8 GPa
T=1200÷1600°C, 4 h

FIB litography +

standard lithography with Al masks

Nitrogen implantation for contact pads

Al etching + thermal annealing

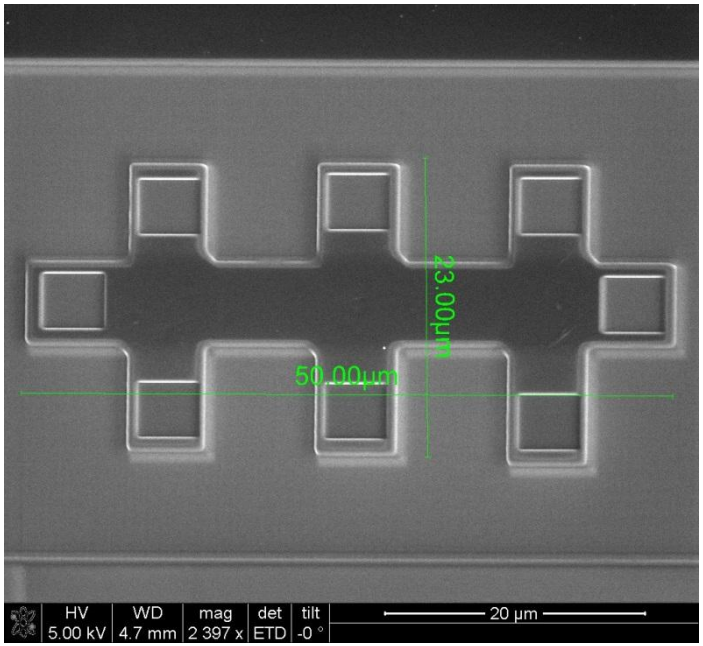

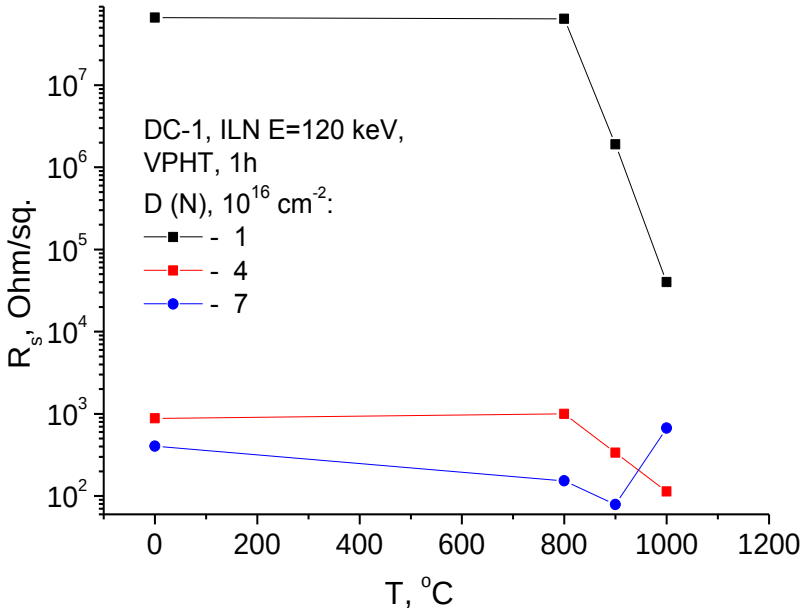

Variable range hopping mechanism of conductivity

$S(T)=S0*T^{-1/2}*\exp[-(T0/T)^{1/4}]$
$T0=16/a^3*k*N(E_F)$
a – radius of hopping site
sp2 bond – a=1.2 nm

When conductivity becomes metallic? Reznik et al. This happens when density of states $N(E_F)$ reaches the value $N_0(E_F)$ determined by the relation $N_0(E_F)*a^3=1$, i.e.
$N_0(E_F)=1/a^3=6\times10^{20}$ states/(eV*cm^3) for a=1.2 nm

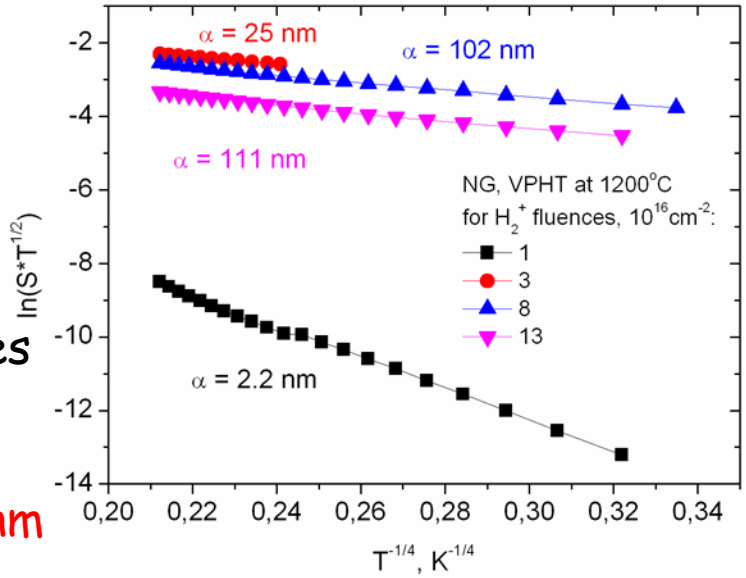

Semimetallic mechanism of conductivity

Quantum correction* due to e-e interaction in diffusion channel:

$$\sigma(T)=\sigma(0)+\Delta\sigma_{e\text{-}e}(T)=\sigma(0)+\beta\cdot T^{1/3}$$

If there is $\sigma(0)<0$ for degenerate semiconductors in cryogenic T-range, then the conductivity has nonmetallic character, i.e. below MIT, but if $\sigma(0)>0$ then the conductivity is quasimetallic after 1200°C or above MIT.

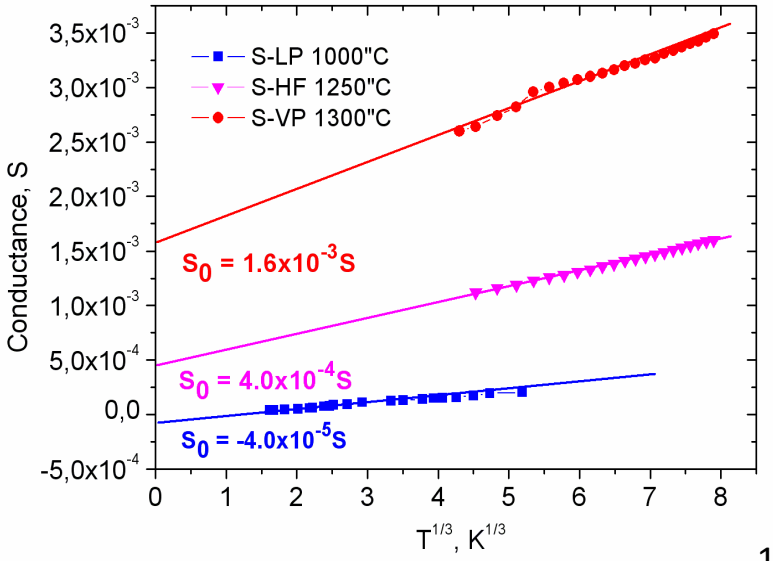

240 & 32 nm membrane from diamond-graphite-diamond (DGD) heterostructures produced by N^+ & H_2^+ II

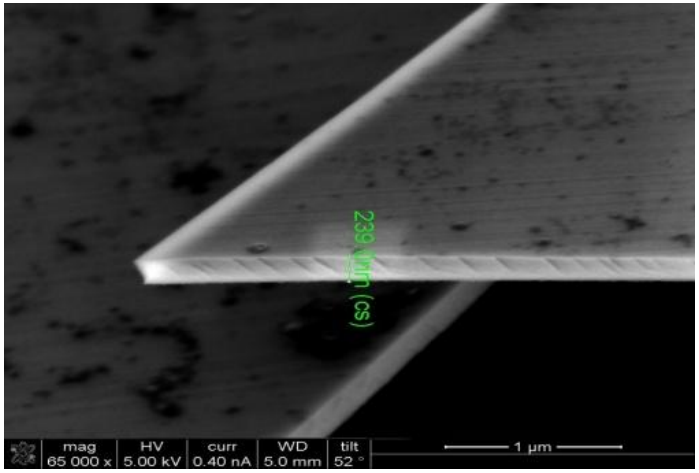

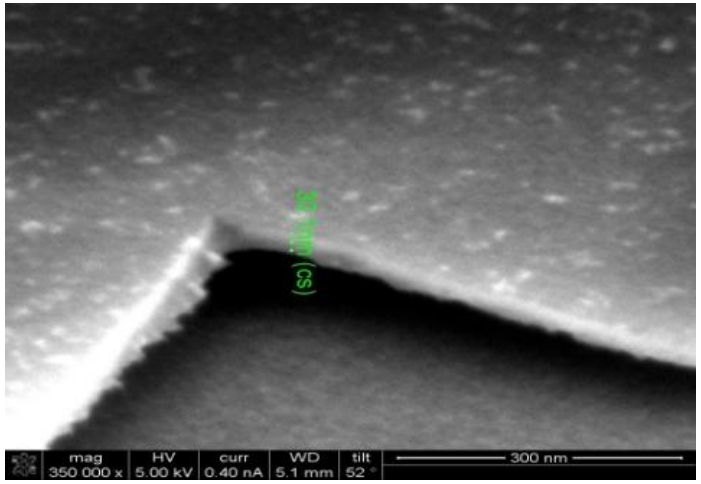

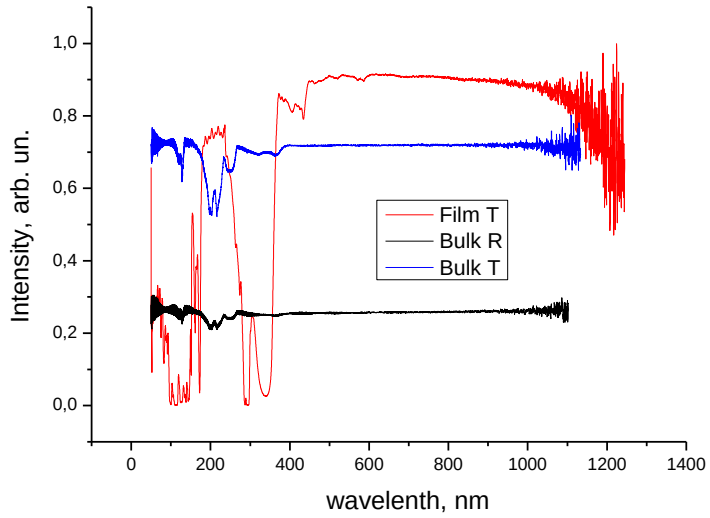

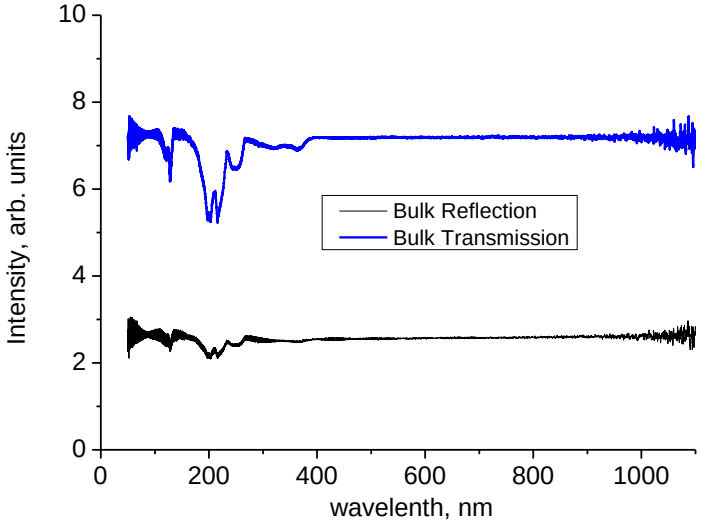

Absorption bands at UV 100 and 300 nm indicate a presence of graphite inclusions after 1600°C,

*V.P. Popov et al. AIP Conf. Proceed., 2012

240 nm membranes from diamond-graphite-diamond heterostructures produced by $(N^+ + H_2^+)II$ + HPHT + Anodic Etching

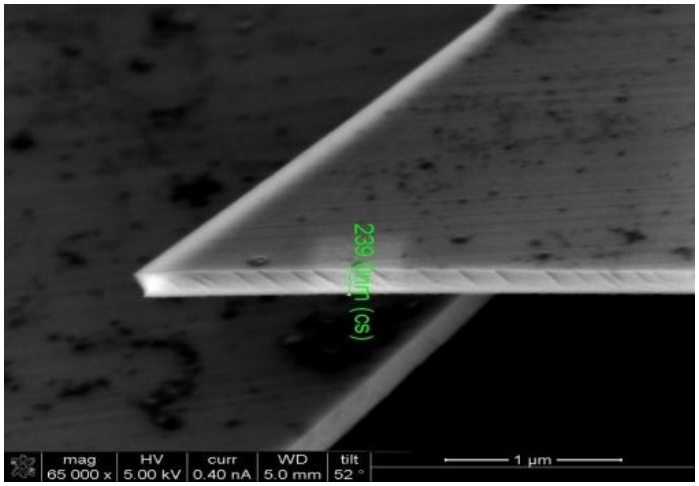

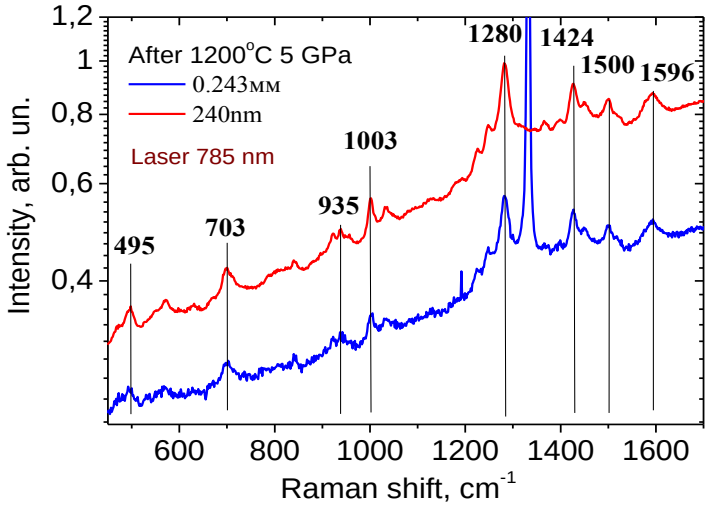

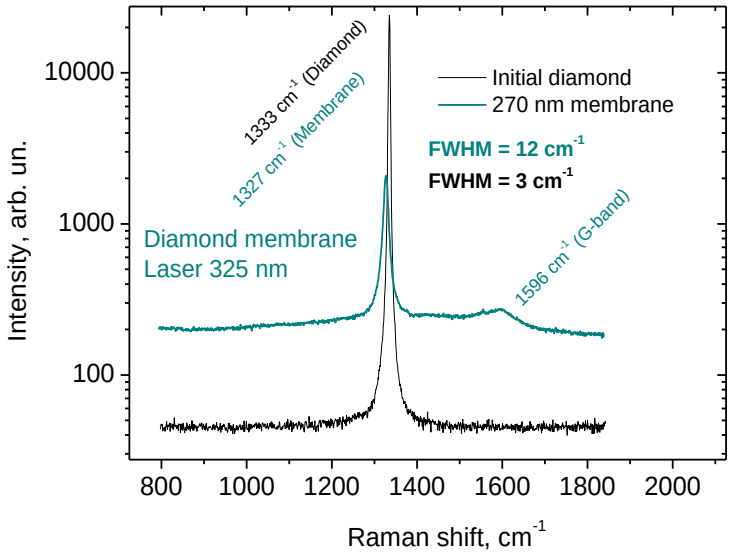

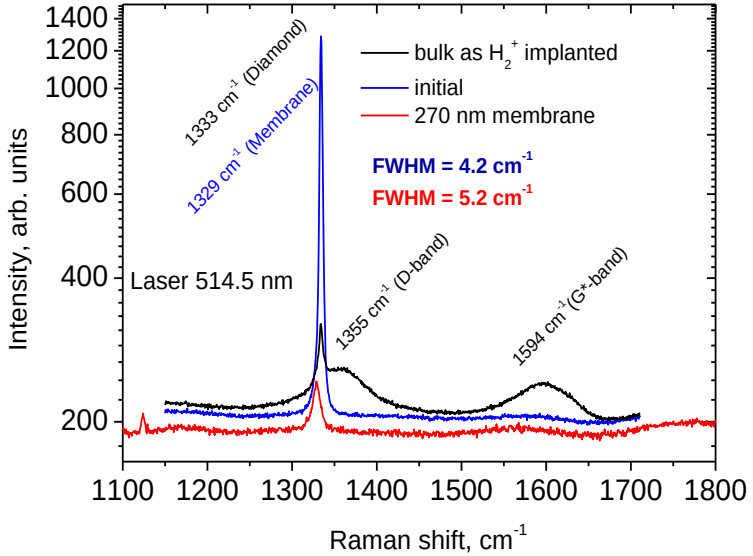

No other PL lines at laser excitation at $\lambda_{ex} \leq 514.5$ nm after 1600°C, only small G*-line and four times larger FWHM for UV RS due to residual stresses*

V.P. Popov *et al.* Int. J. Nanotechnol., 12, 226 , 2015.

Tareeva, *et al.* Bull. Lebedev Phys. Inst. 44 (2017) 210

Bonding of diamond 30 nm film to PMMA or glass substrate

Hydrogen molecule fluence $\Phi = 8 \times 10^{16}$ см$^{-2}$ after HPHT annealing at 1200°C 1h

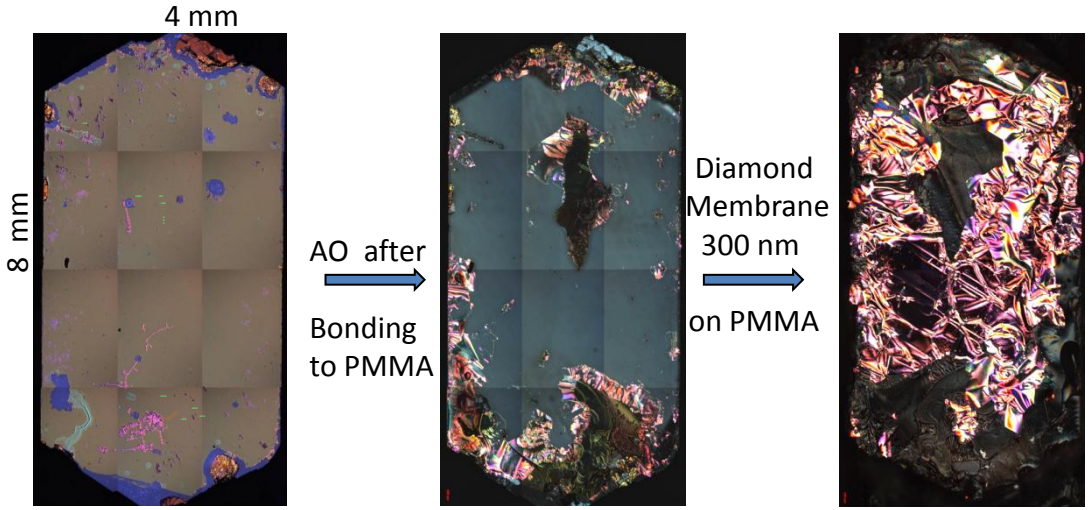

HII: H_2^+ 50 keV, 8×10^{16} cm^{-2}, HPHT, 1200°C, 5GPa 2h,

AO of 110 nm Gl-C and transfer of 290 nm diamond on PMMA substrate (delamination by residual stress in diamond membrane)

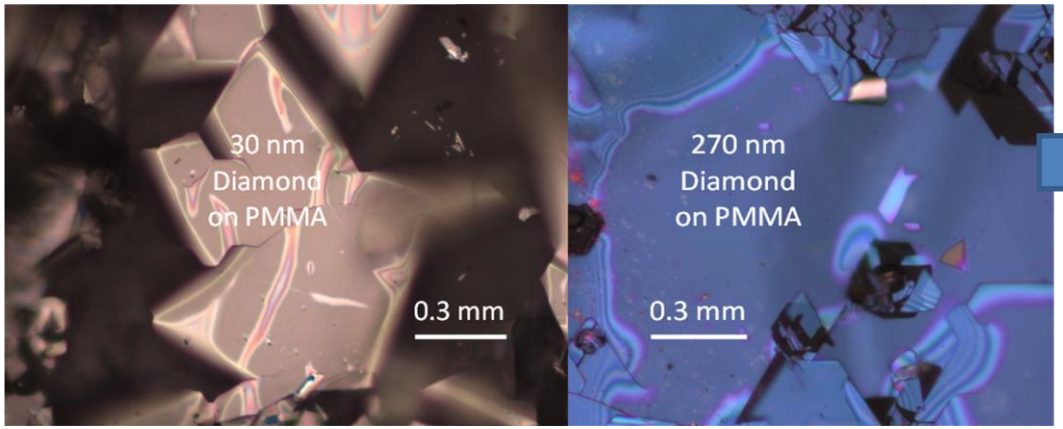

Outlook

1. Motivation for Diamond Electronics
2. Diamond-Graphite-Diamond by II & Lift-off Process
3. **Diamond Junction & Field Effect Transistors J-, MISFET**
4. Sensing by Membranes & NV Defects in Nanostructures
5. Conclusion

Diamond vs. Silicon p-n Junctions

Measured I-V characteristics of p-n mesa junctions at RT after 1200°C 4 GPa

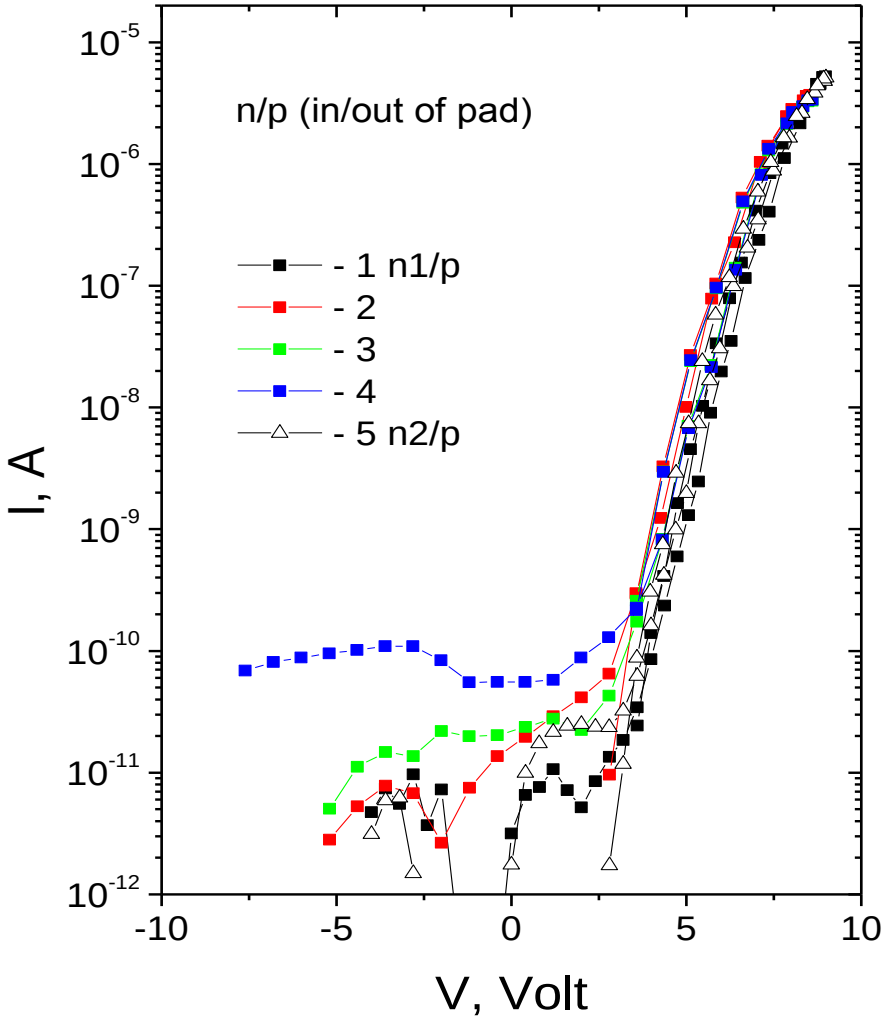

I-V characteristics of equally doped p-n junctions at RT simulated by TCAD Synopsys

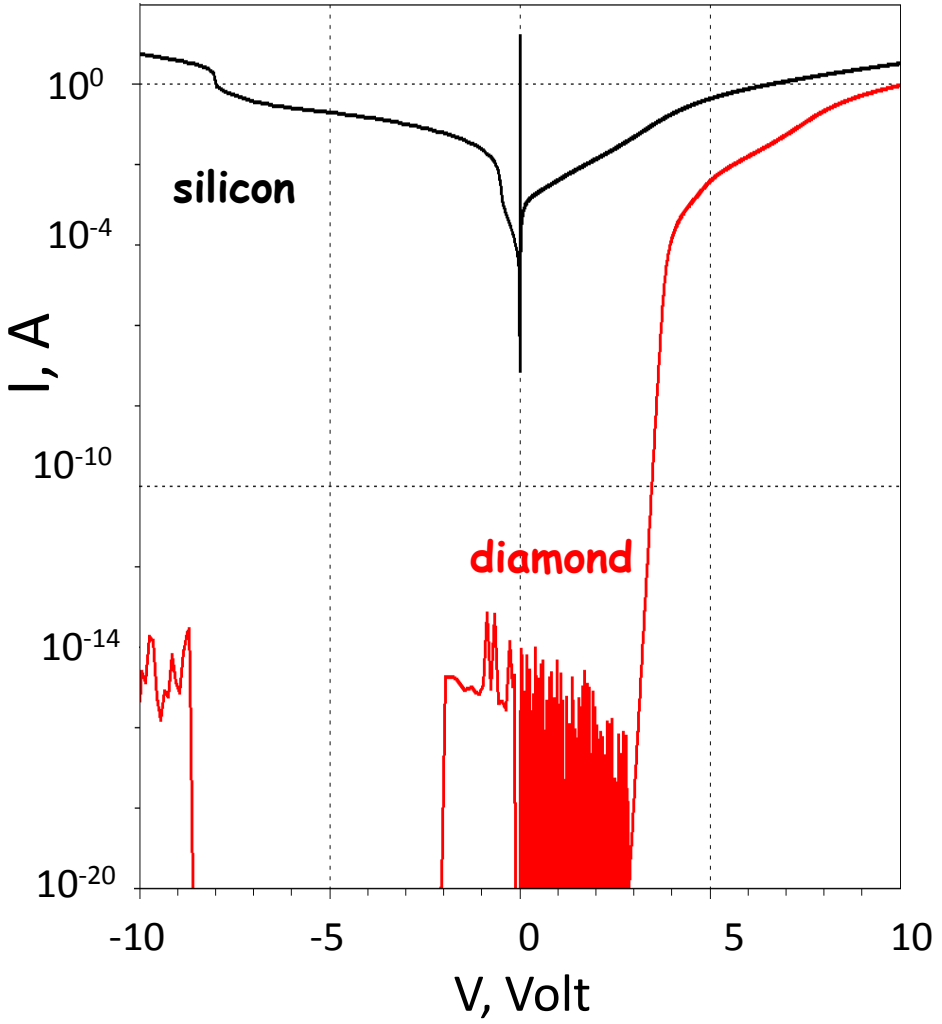

Design of Diamond Hetero or Schottki Barrier n-MISFET

Diamond body. The drain and source are made from **Al,Pt Schottki or n^+-type** ($10^{19}cm^{-2}$) **silicon carbide Hetero Barrier** and located at the edges of the diamond body (in one plane):

- Full length of the transistor is 200 nm.
- **The length of the gate is 100 nm.**
- The length of the channel is 104 нм.
- The length of drain & source is 20 nm.
- **The thickness of diamond layer is 20 nm.**
- The thickness of the gate oxide is 2 нм.
- Top aluminum (Al) gate.
- The back oxide thickness is 20 nm on Al plate.

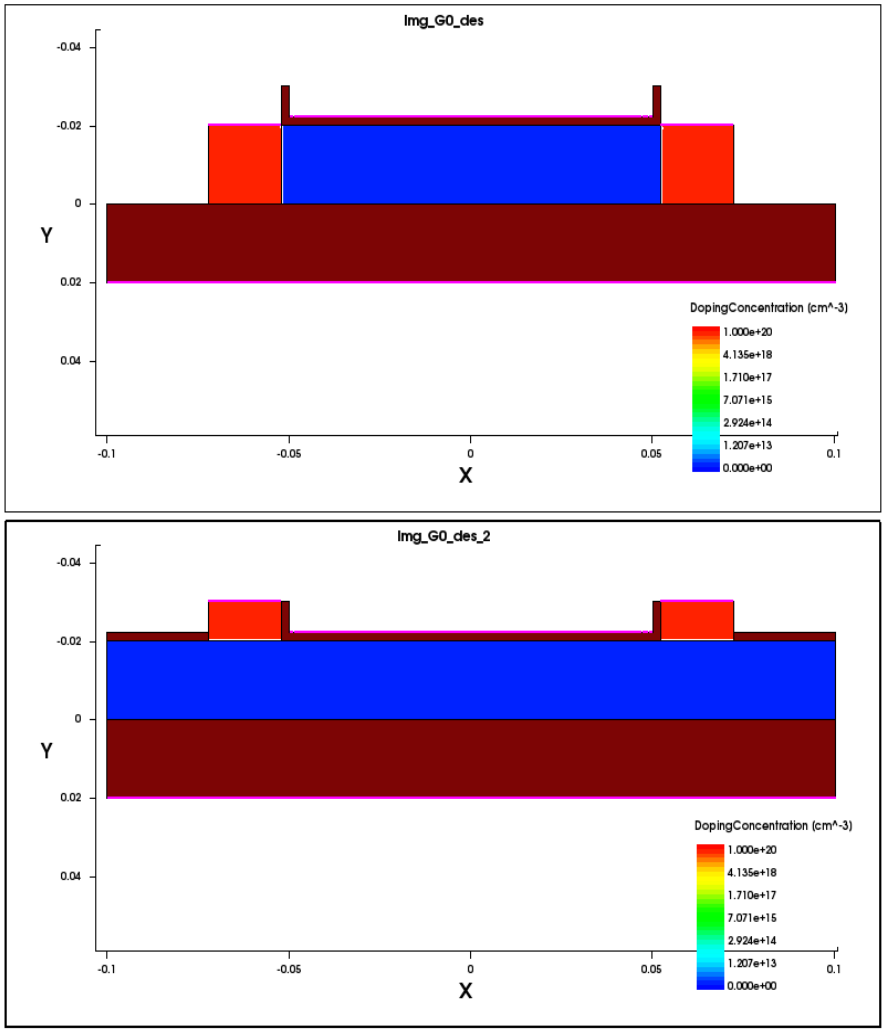

Electron Density in Diamond FETs with Schottki Barriers

I-V characteristics of SB MISFET at RT simulated by TCAD Synopsys

No large difference in SB MISFET for four different parameter sets by TCAD Synopsys

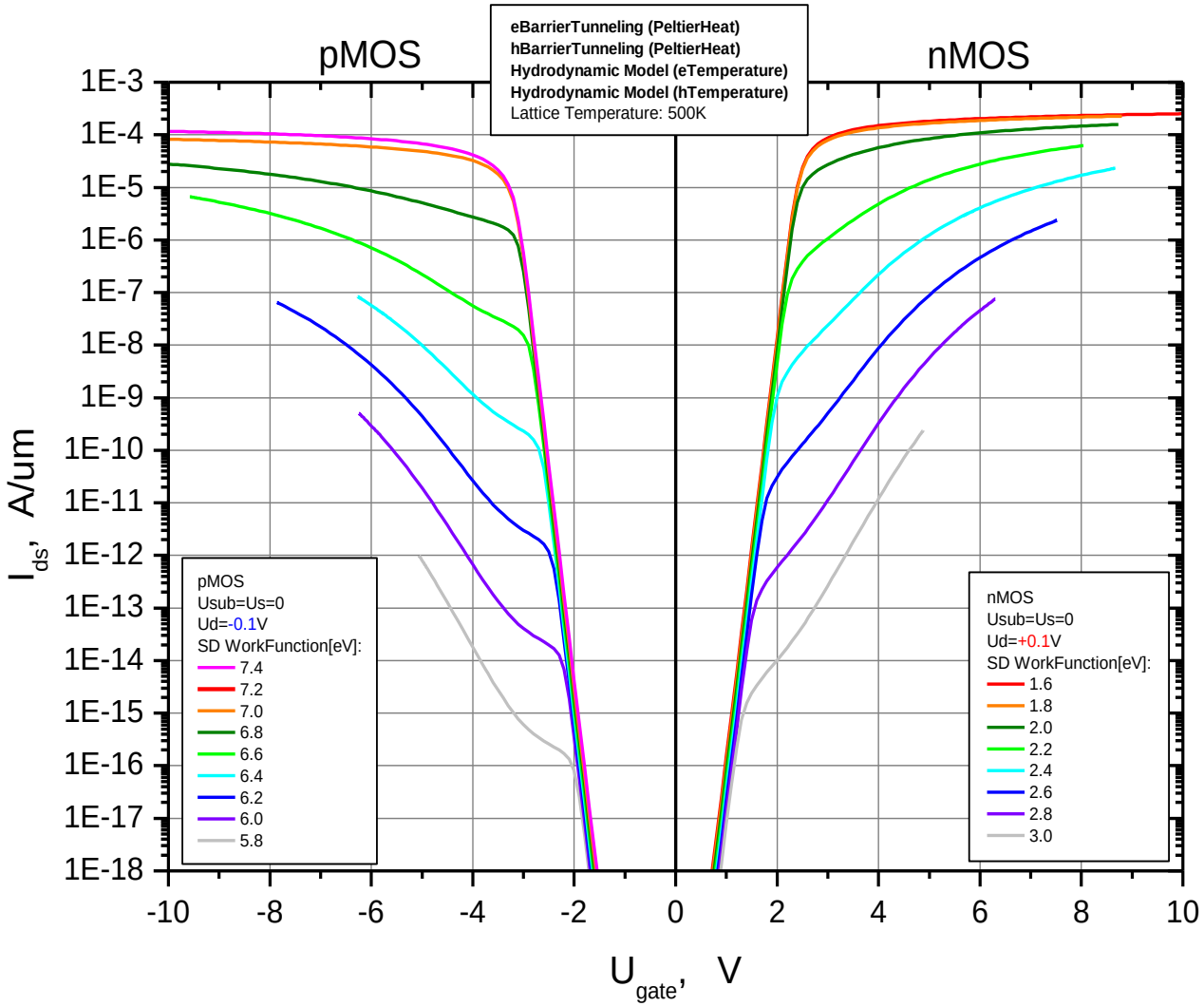

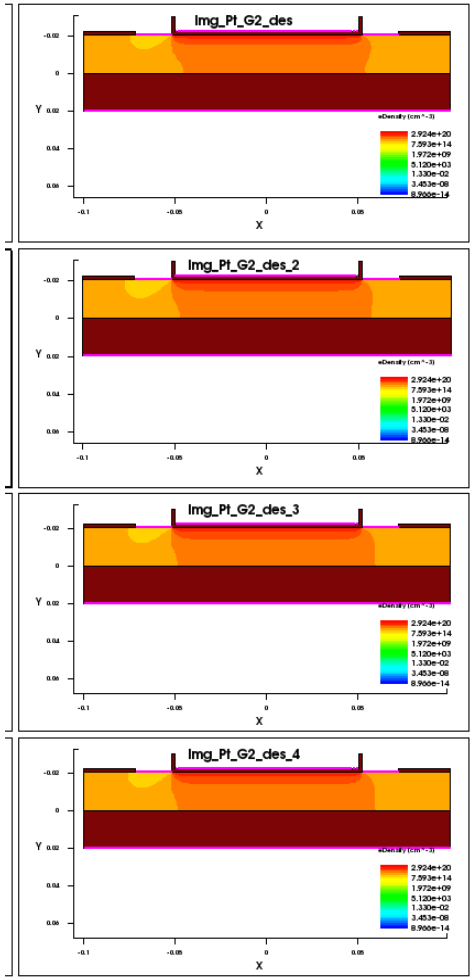

Ion = 10mA/mm: Eχ<-6.9 eV SB p-MISFET Eχ>-1.8 eV for SB p-MISFET at Vg>+2 V

E-Bands & Current Density in Diamond Hetero n-MISFET

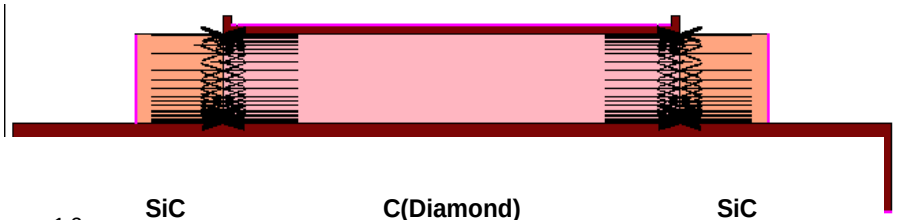

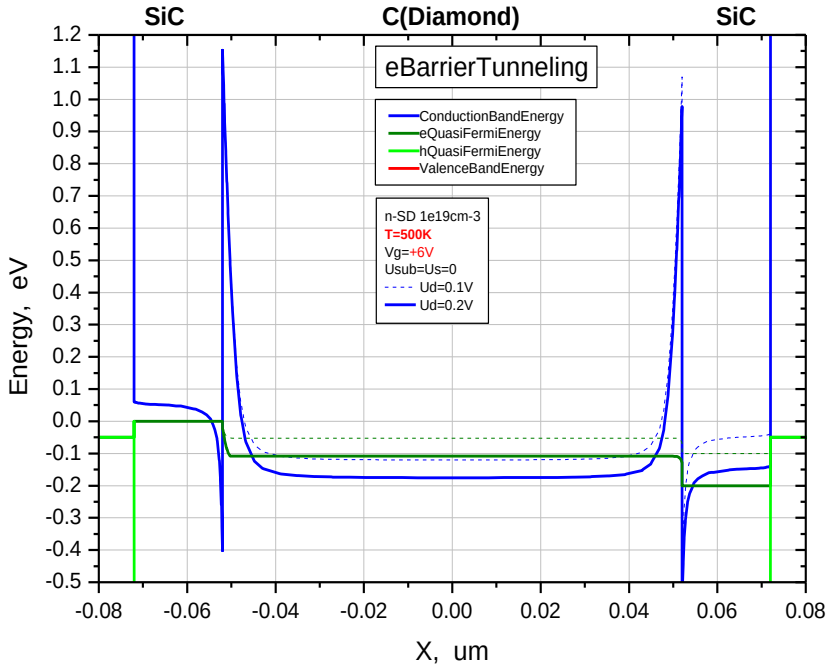

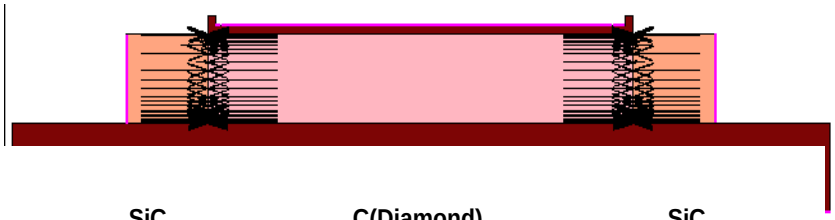

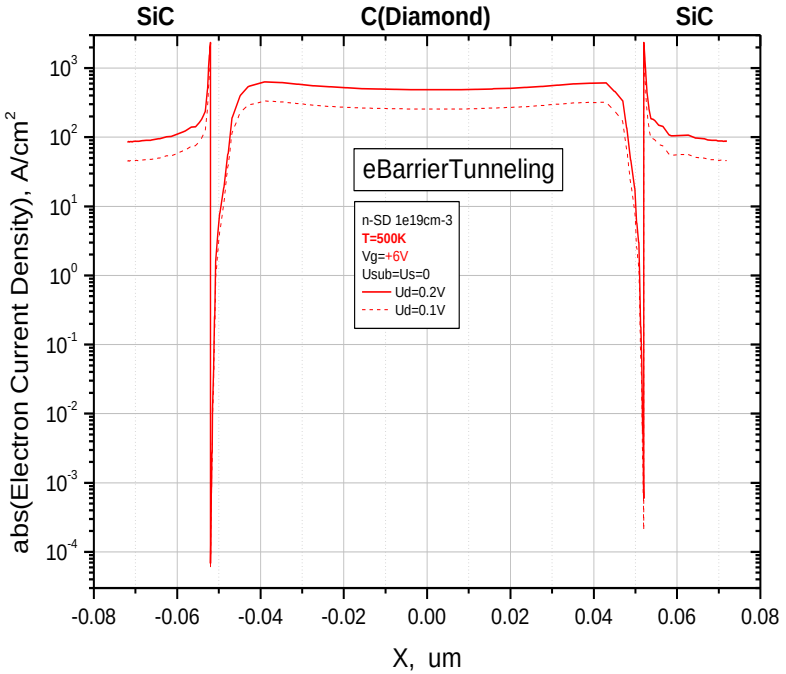

Bottom of conduction band and Electron Density at +1 nm under the surface

Heterobarrier n-MISFET vs. inversion channel p-MOSFET

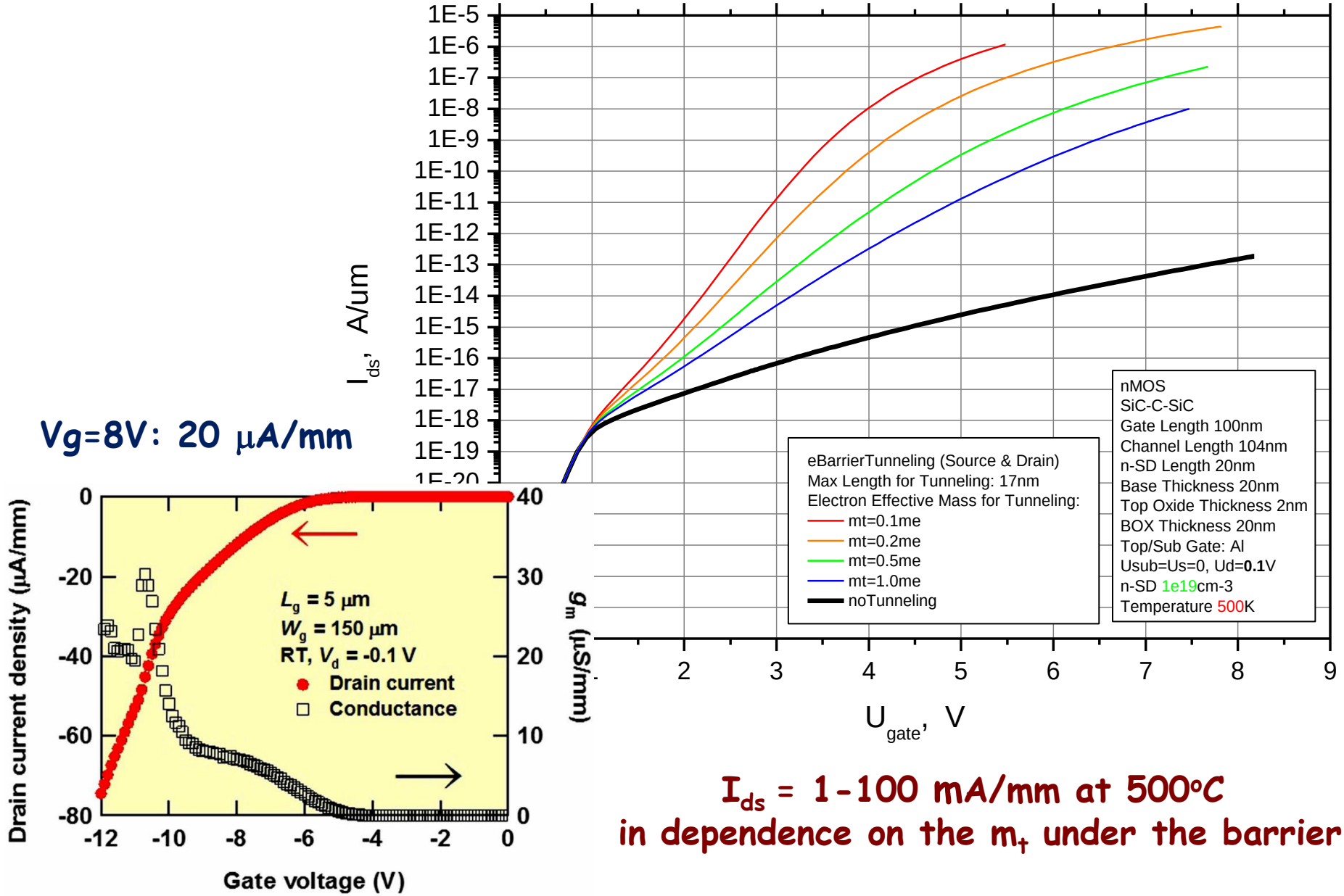

Vg=8V: 20 μA/mm

I_{ds} = 1-100 mA/mm at 500°C
in dependence on the m_t under the barrier

Matsumoto, T. *et al. Sci. Rep.* ***6*** *(2016) 31585*

Heterobarrier n-MISFET vs. inversion channel p-MOSFET

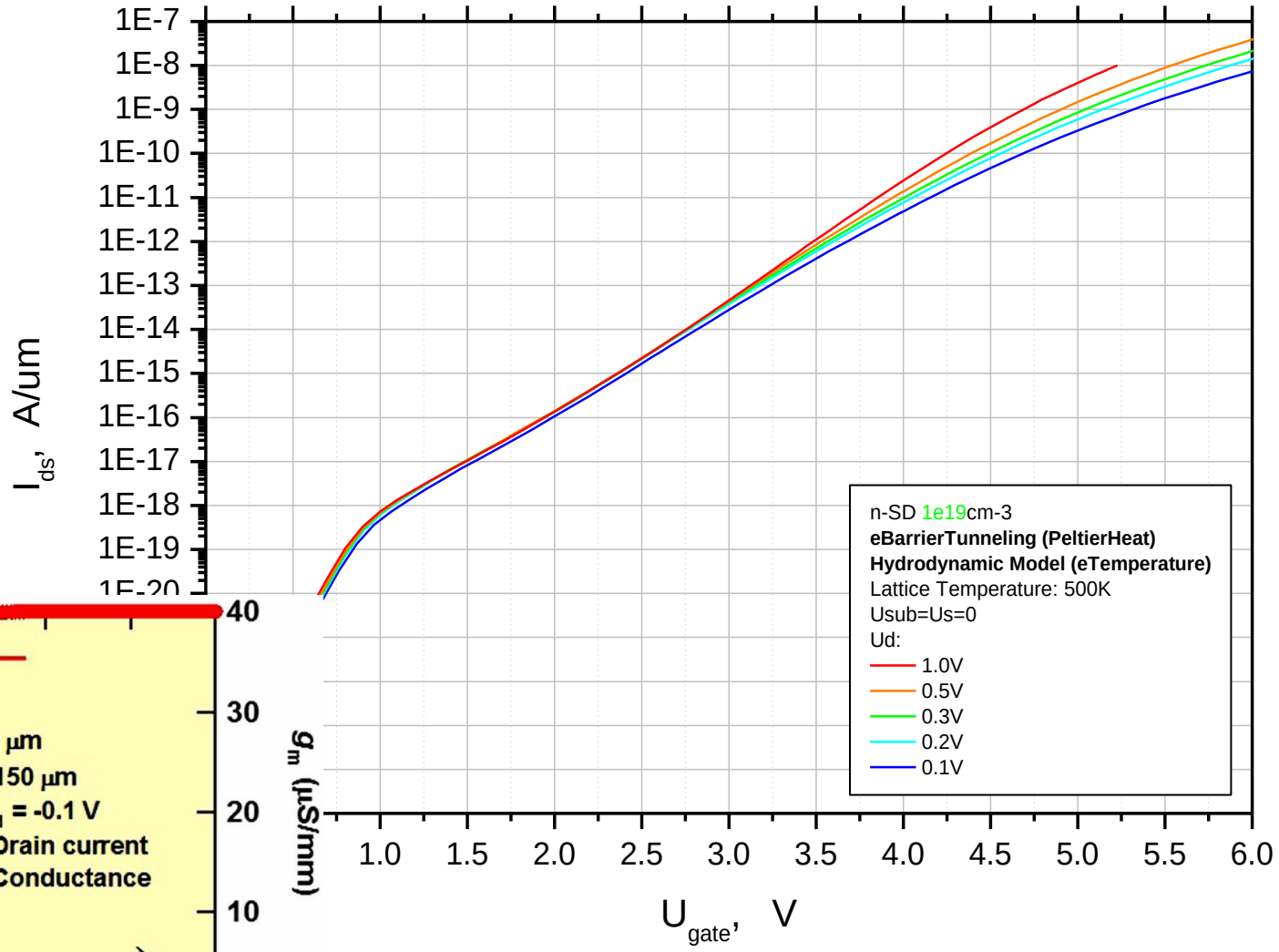

Vg=6V: 5 μA/mm

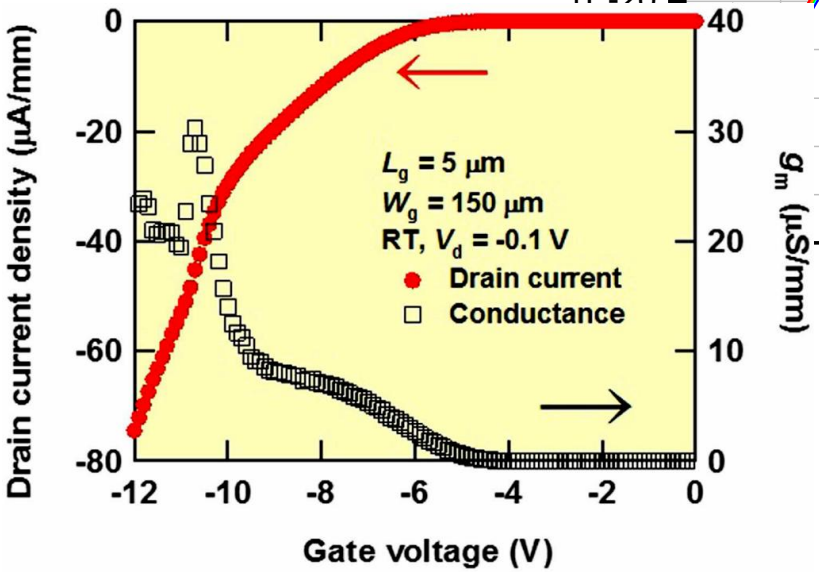

I_{ds} = 100 mA/mm at 500°C

But we need to account correctly the dependence μ = μ(E)

Matsumoto, T. *et al. Sci. Rep.* ***6*** *(2016) 31585*

Heterobarrier p-JFET with n-type g-C3N4 mesh

CN-heterojunctions with Ioff/Ion ~ 10^{-3}

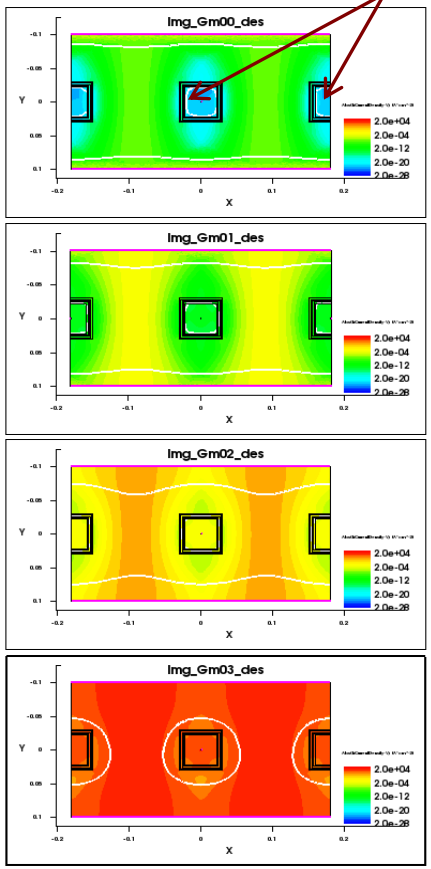

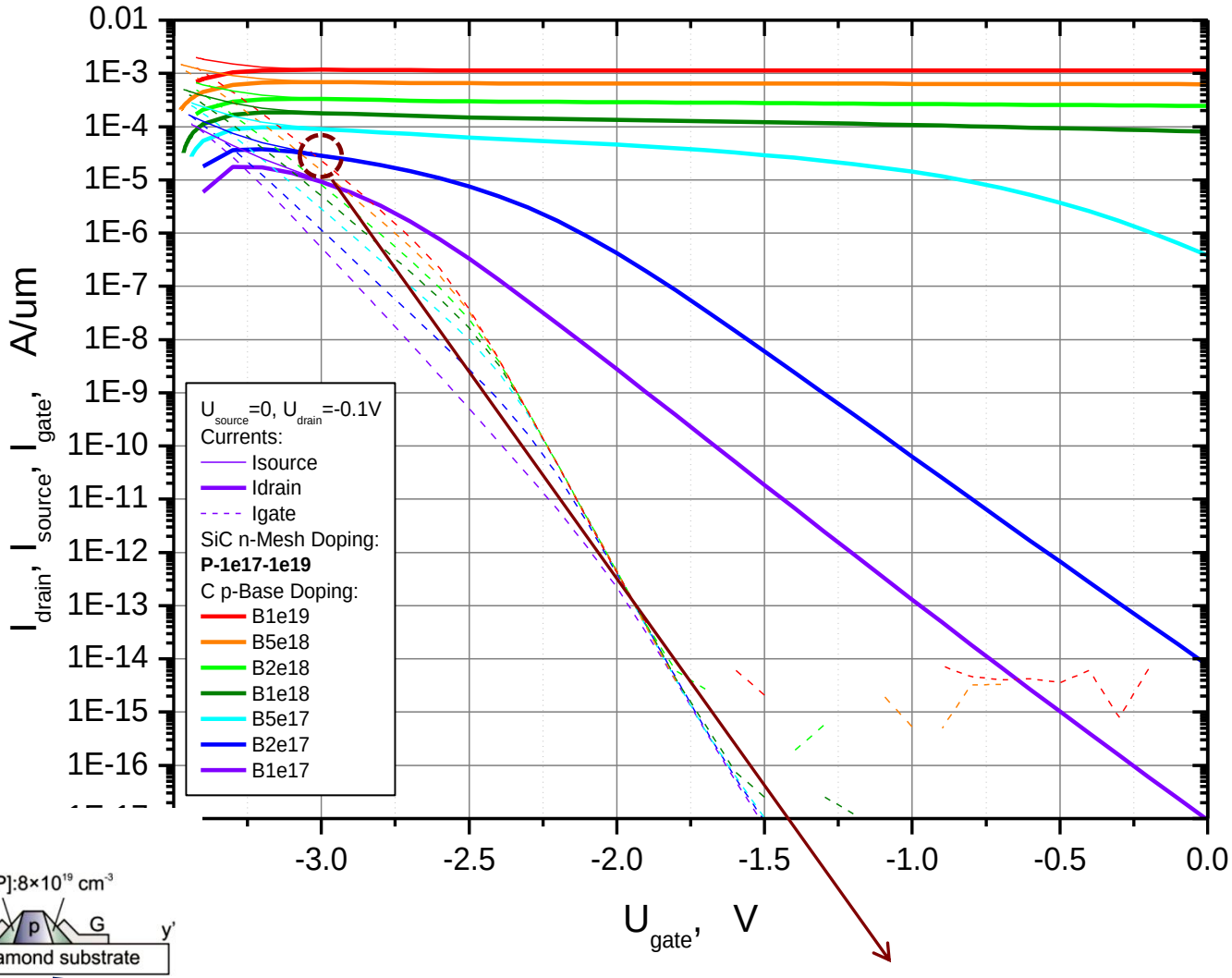

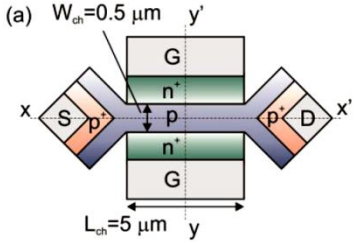

Vg=-3V: 50μA/mm vs. 50mA/mm at 500K

**Iwasaki T. et al. JEDS 5 (2016) 2624301*

Outlook

1. Motivation for Diamond Electronics
2. Diamond-Graphite-Diamond by II & Lift-off Process
3. Diamond Junction & Field Effect Transistors (J- & FET's)
4. **Sensing by Membranes & NV Defects in Nanostructures**
5. Conclusion

Diamond & Multigraphene Membranes as Silicon FET gate

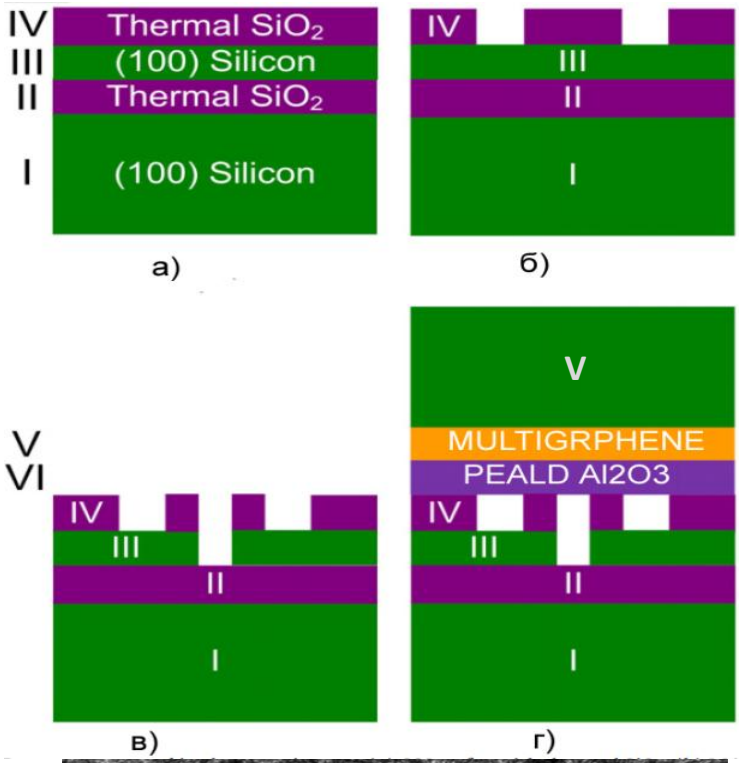

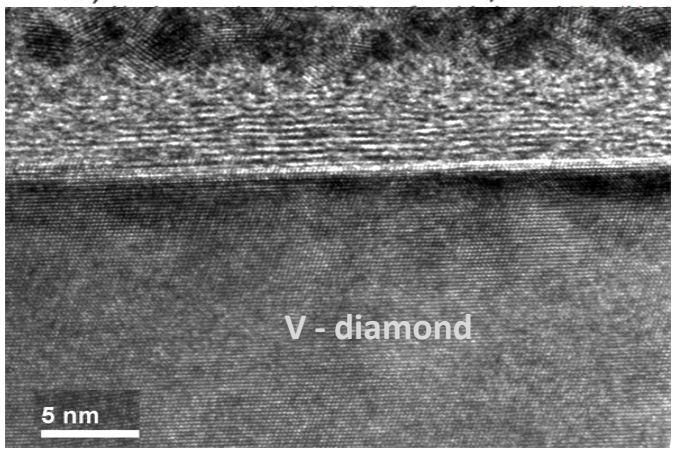

I-V characteristics of membrane gated FET with three gate lengths simulated by TCAD Synopsys

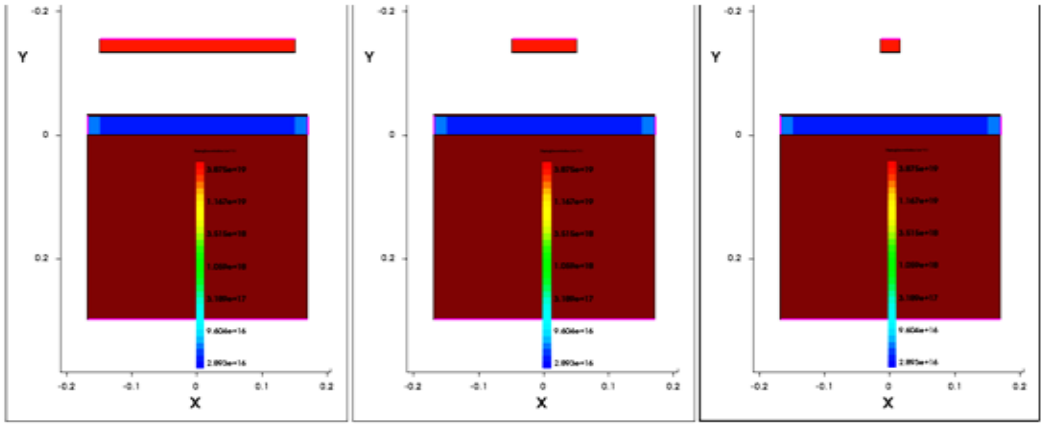

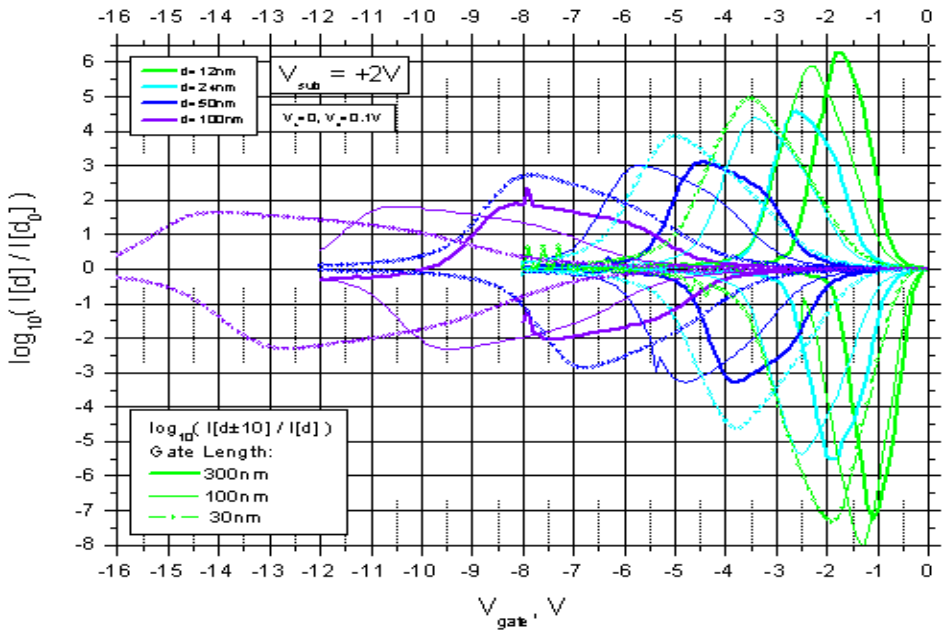

Stark Effect at NV⁻centers in forward biased p-i-n diode

Exciton luminescence (V_{FB}=35 V)

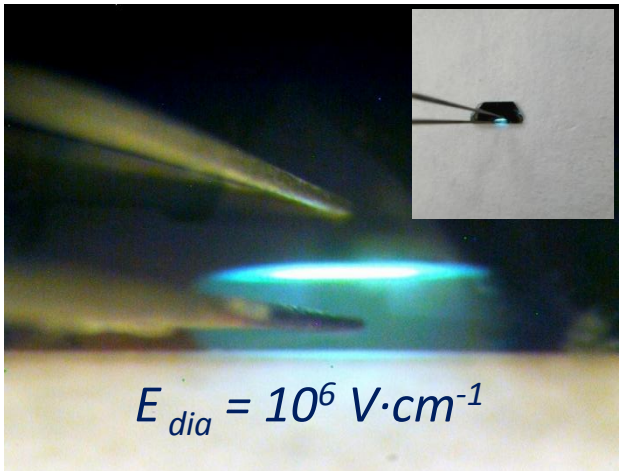

lateral p-n junction

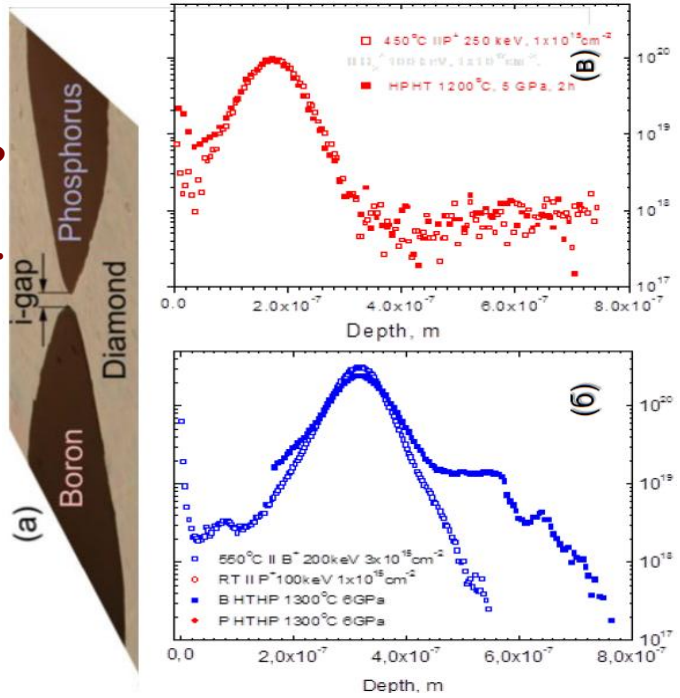

Splitting in Stark shift for 2 NV⁻ groups

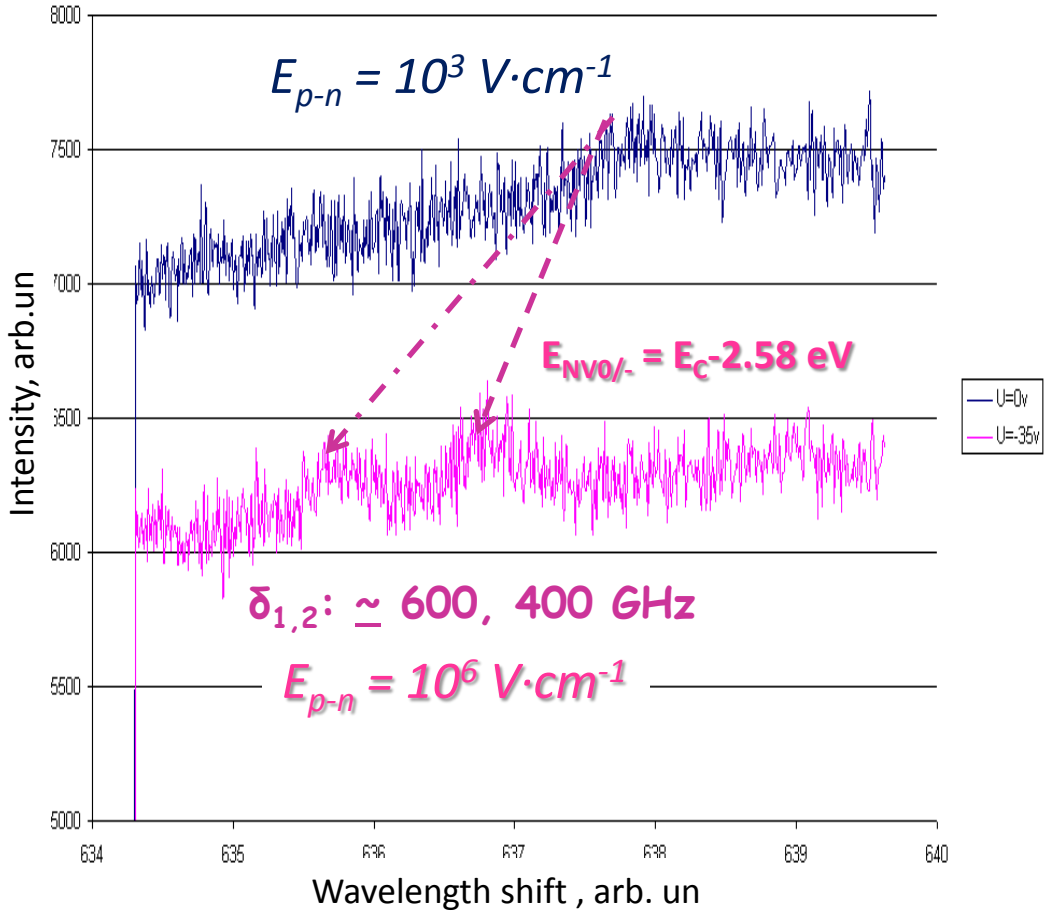

The splitting allows to control of the spins in differently oriented NV- groups along <111> axes

V Popov. *et al.* Proceed. of ISI-2015 Int. Conf., Moscow, 2 (2015) 13-19

ODMR of NV's in 300 nm N^+ implanted layer at high temperature

$$H = D\,[S_Z^2 - S(S+1)/3] + \gamma\,[\mathbf{B} + \mathbf{b}(t)]\cdot\mathbf{S} + E(S_X^2 - S_Y^2),$$

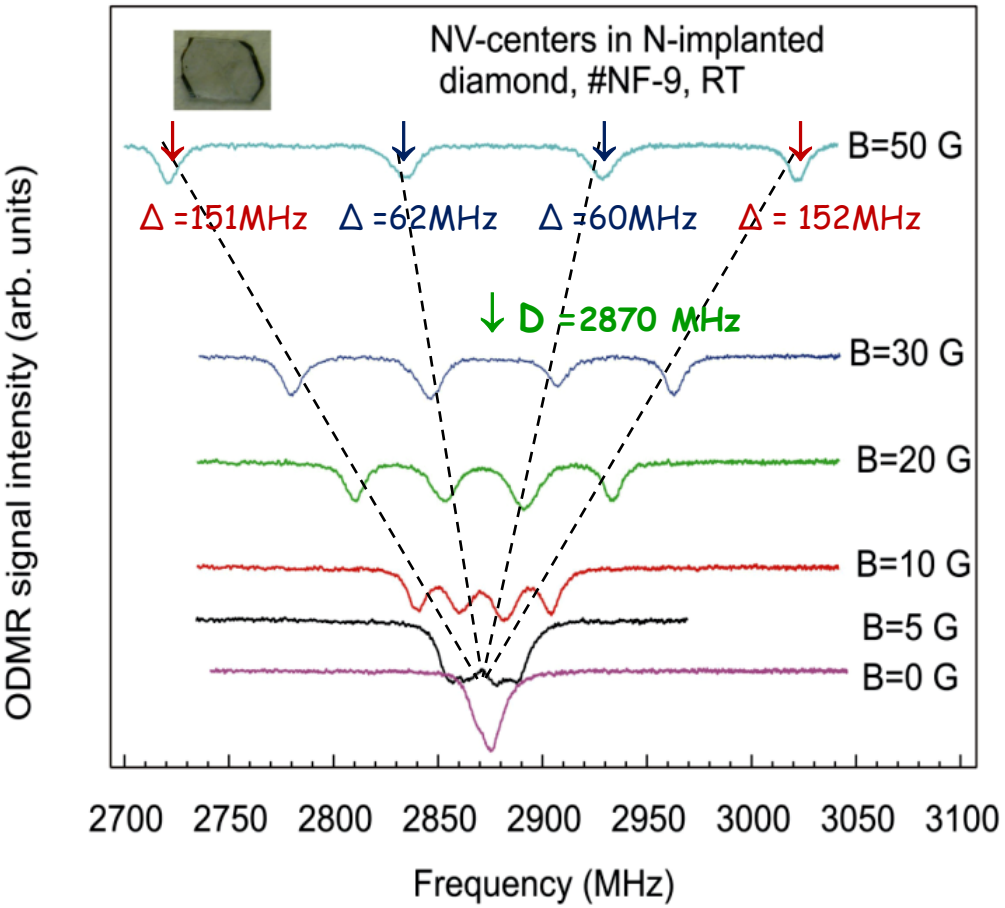

No hyperfine splitting* for NII:

(3.1 MHz)/(9.5 MHz) -> δ = 6.3 MHz

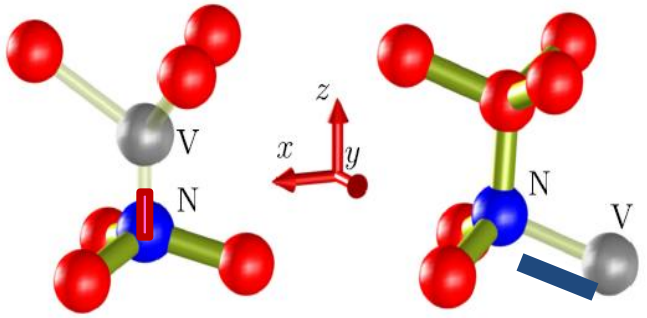

45% of the NV's are ⊥ to the surface***

If transverse spin-relaxation time T_2^* is:

$T_2^* = 1/(\pi\delta) = 52$ ns

Spin-relaxation time T due to dipolar coupling is:

$T_{NV} \simeq 1/[(g_s\mu_B)^2 n_{NV}] = 700$ ns

$T_{NV} \simeq 1/[(g_s\mu_B)^2 n_{Ns}] = 200$ ns

T is limited by high n_{Ns}

Highest T_{NV} ~500 ms for $n_{Ns} = 10^{15}$cm^{-3}:**

$T_{NV} \simeq 1/[(g_s\mu_B)^2 n_{NV}] = 1$ s

$T_{NV} \simeq 1/[(g_s\mu_B)^2 n_{Ns}] = 130$ ms

*T. Yamamoto *et al.* Phys. Rev. B **90,** 081117(R) (2014).

**N.Bar-Gill *et al*. Nat. Commun. 4:1743 (2013).

***T.Karin, *et al.* Appl. Phys. Lett. 105, 053106 (2014).

V Popov. *et al.* Proceed. of ISI-2015 Int. Conf., Moscow, 2 (2015) 13-19.

On-Crystal Quantum Network *from M. Lukin group. P.R.L. 110 (2013) 067601*

Magnetic dipole coupled spin arrays $E_{md} \sim 1/d^3 \rightarrow d \sim \sqrt[3]{T_2}$

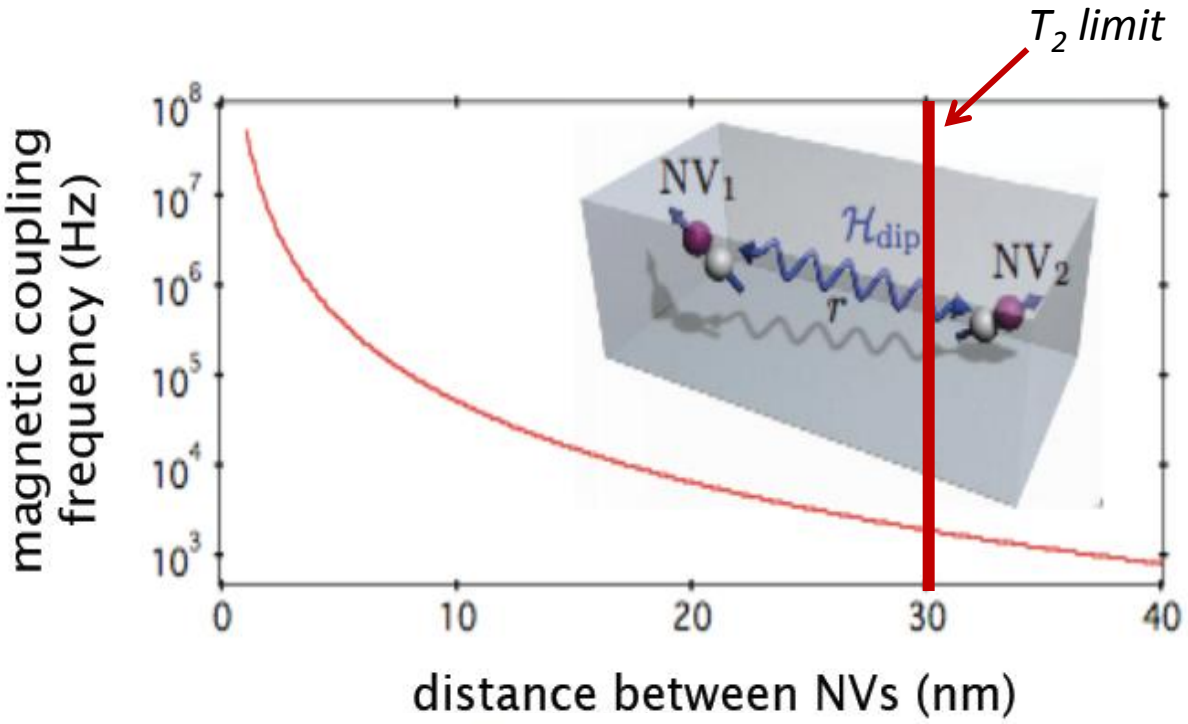

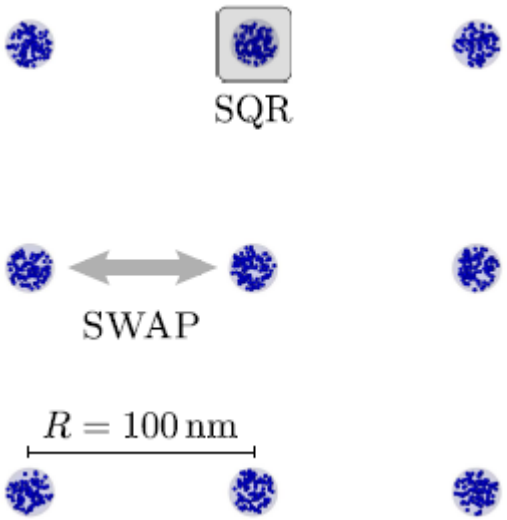

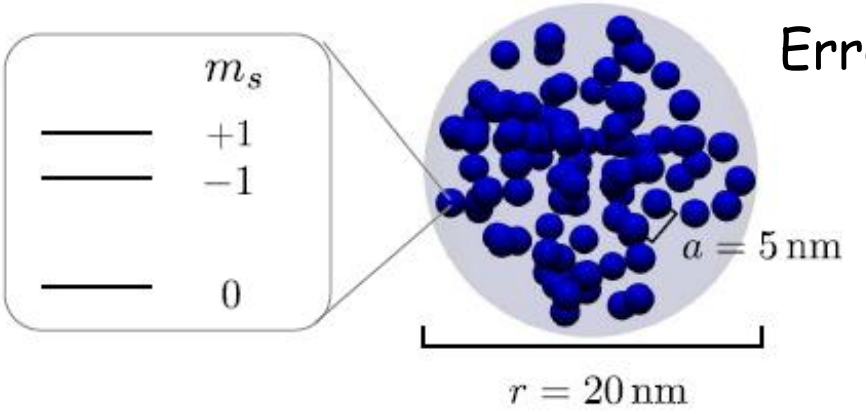

Error in collectively enhanced quantum gates

$\varepsilon = 1 - \exp[-(4t_\pi/T_2^*)^3]$

For $\varepsilon = 10^{-4} \rightarrow T_2^* = 11$ ms

PL Peaks of NV ensembles in Ar_{27} Cluster Ion Implanted Diamond

The probability to find analogical or other charged centers with content [C_{Ns}] = 2.5x10^{13} cm^{-3} in neighborhood of 10 nm layer on the distance r and determines as **exp(-π[C_{Ns}]R^2) = 1/2.**
Then the distance R is equal to R ≈ 0.47([C])$^{-1/2}$ = **1x10^{-6} cm =10 nm**

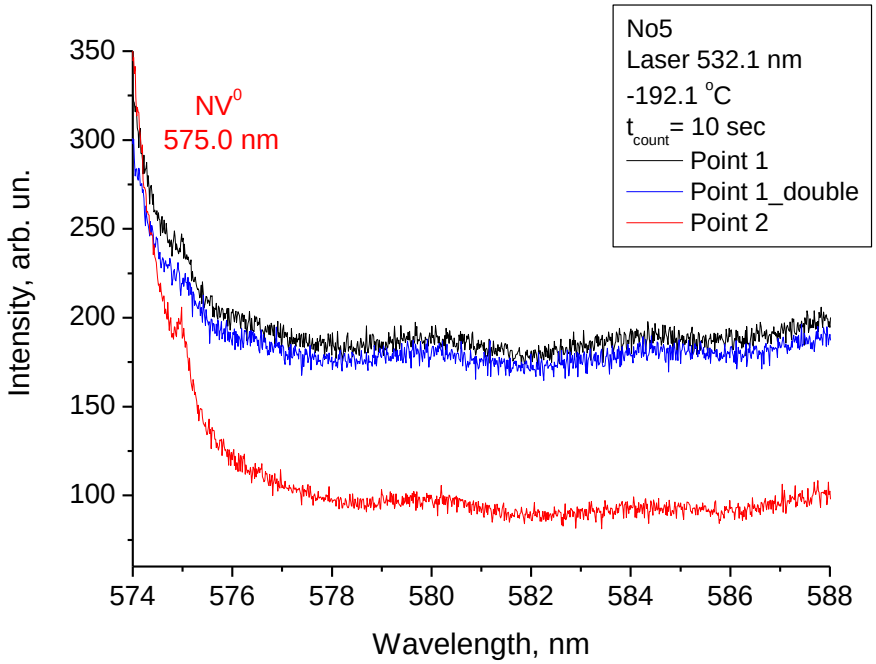

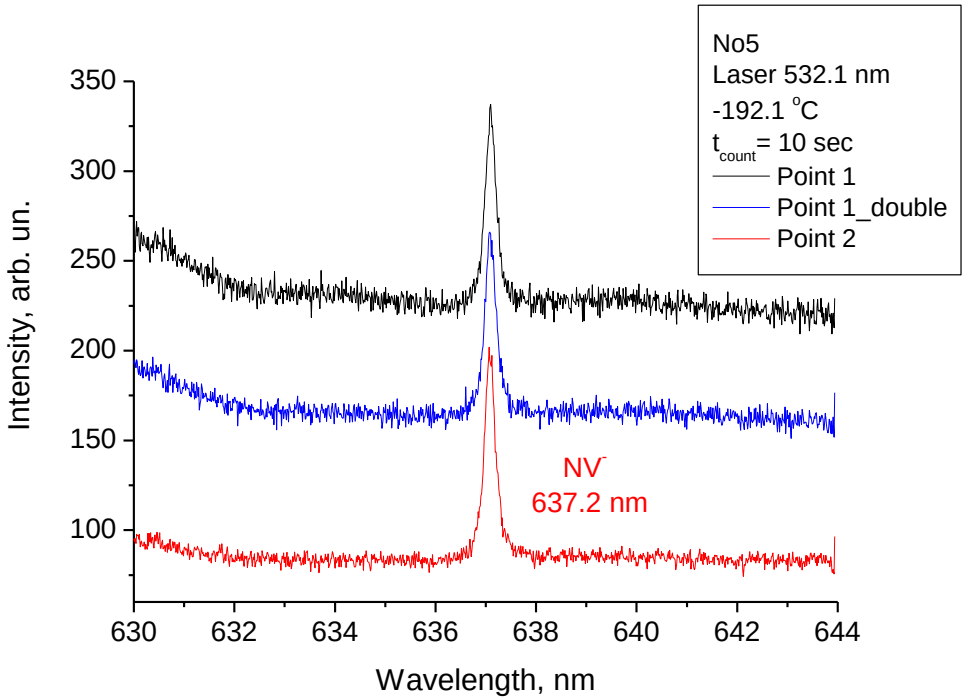

FWHM for 0.2-20ppm NV's is the same for bulk, HNI & HII diamond

Visible PL at 575 and 637 nm of NV^0 & NV$^-$ with content [C_{NV}] = 5x10^{13} cm^{-3} at LNT

FWHM of NV$^-$ is δ=170 GHz or 230±10 pm instead of δ=30 GHz for single NV$^-$

NV's mainly in clusters!

V.P. Popov, et al. . ICW-2010, Kyoto 2010

PL CLM of NV ensembles in Ar_{27} Cluster Ion Implanted Diamond

The probability to find analogical or other charged centers with content [C] = 2.5×10^{13} cm^{-2} in neighborhood on the distance r and determines as **$\exp(-\pi[C]R^{\wedge}2) = 1/2$.**
Then the distance R is equal to $R \approx 0.47([C])^{-1/2}$ = **1×10^{-6} cm =10 nm (anneal. 850°C)**

425µm

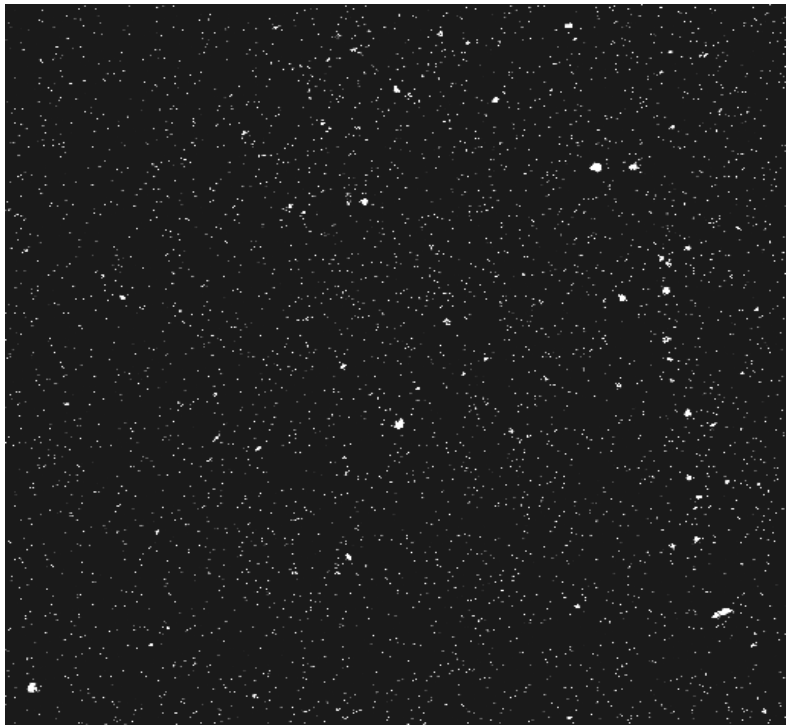

425µm

Number of NV centers в in spice - $N_{NV's}$:

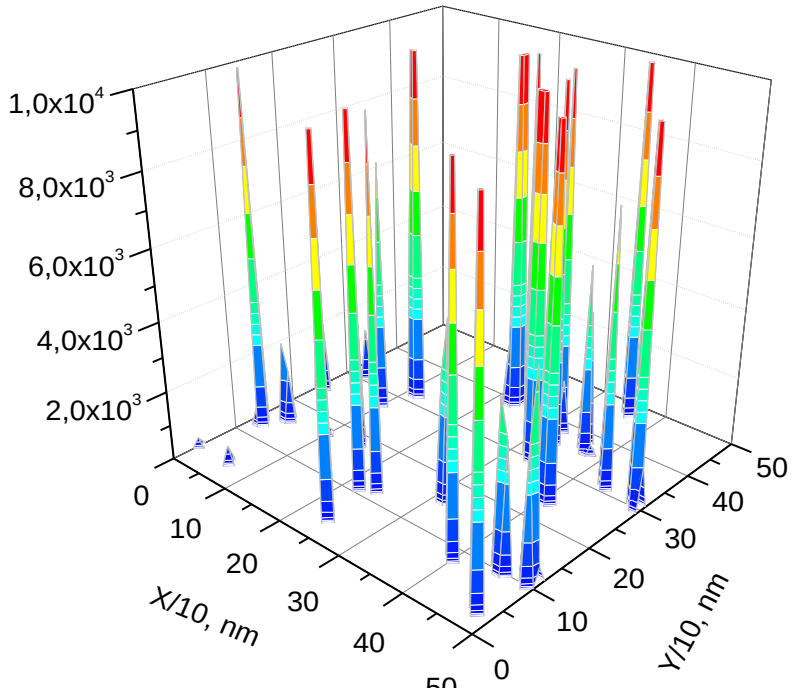

1	25
2	50
3	100
4	150
5	200
...	...
10	

NV^- ensemble spots with area content $[C_{NV}]_s$ = 3×10^6 cm^{-2} **or 1/300 of $[N_{Cl}]$!**

Average distance R is equal to $R \approx 0.47([C_{NV}])^{-1/2}$ = **1.6×10^{-4} cm = 1.6 µm at RT**

Solid State Lenses with One NV Ensemble made by Ga^+ FIB

532 nm green laser beam with 300 nm in diameter

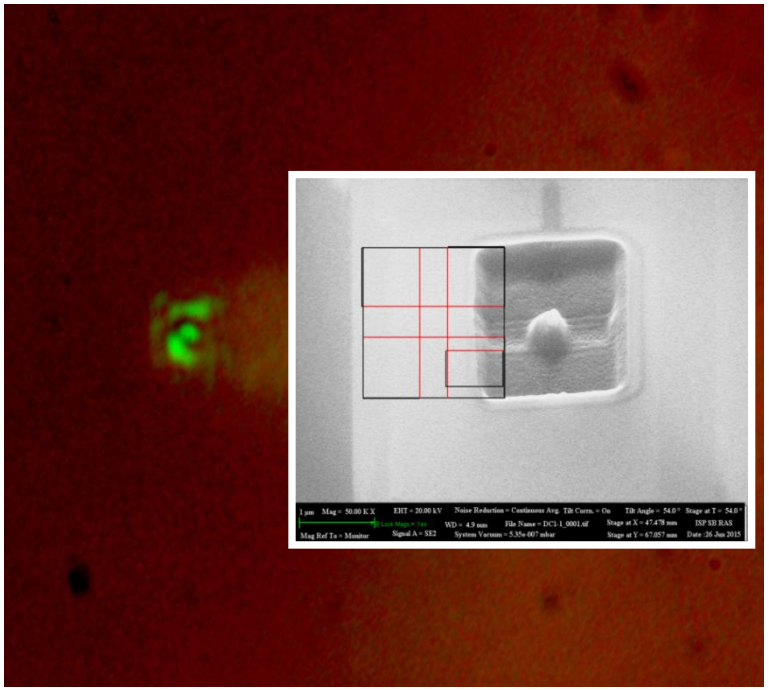

PL increasing for solid state lenses due to a suppression of inner reflection

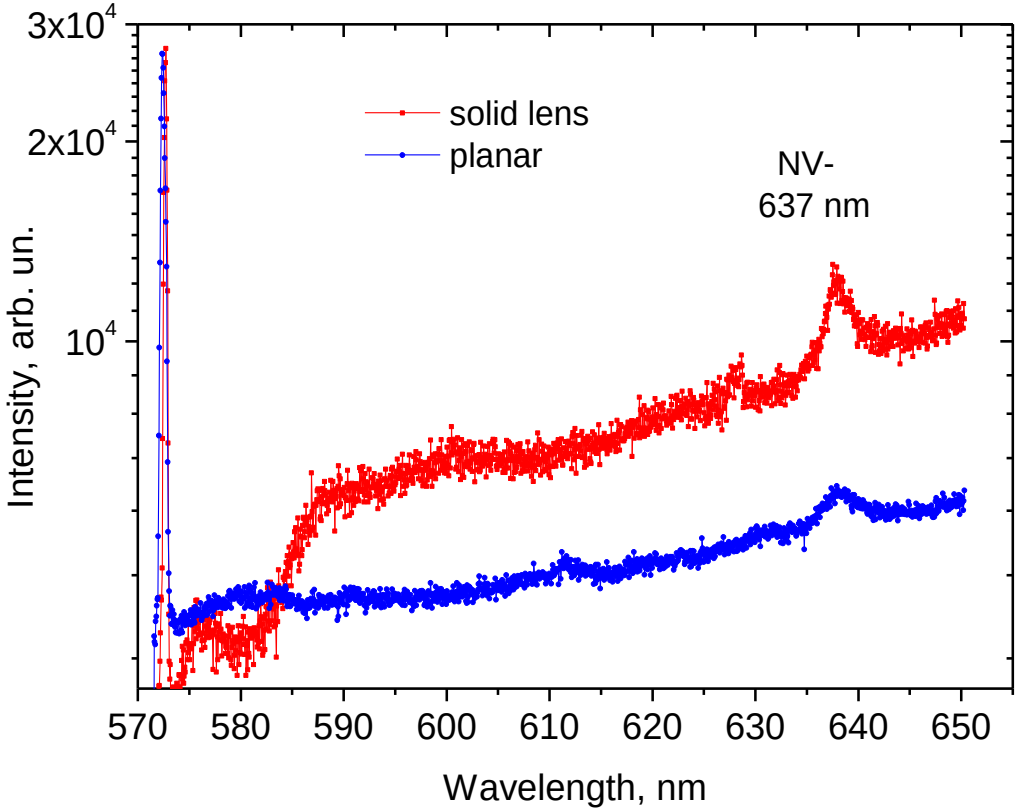

But what is the influence of FIB induced defects ?

$[C_{NV}]_s$ = 3x10⁶ cm⁻² than average content in lens is $\langle N_{NV} \rangle$ = 50 pcs.

5x increase in NV^- PL intensity, but we need a regular matrix !

V.P. Popov et al. RFTT-2015 Conf. Proceed., 2015, 147

ODMR of NV's (~50 pcs) in H⁺II & annealed pillars of 300 nm in the height

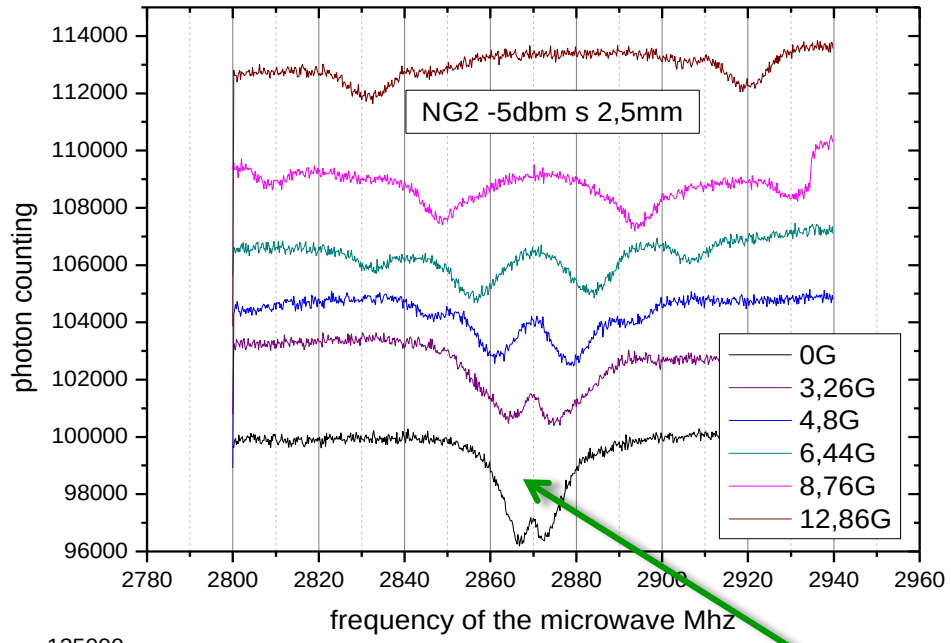

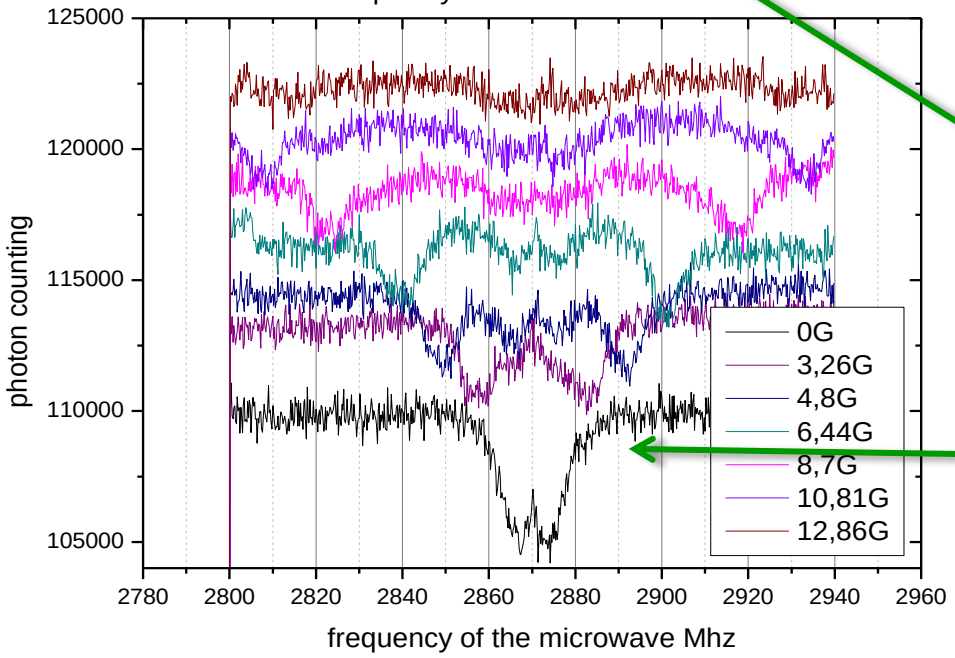

For H⁺II only strain splitting is observed:

(3.1 MHz)/(6.3 MHz) -> δ = 3.2 MHz

If transverse spin relaxation time T_2^* is:

$T_2^* = 1/(\pi\delta) = 100$ ns

Spin-relaxation time T due to dipolar coupling:

$T_{NV} \simeq 1/[(g_s\mu_B)^2 n_{NV}] = 3.5$ µs

$T_{NV} \simeq 1/[(g_s\mu_B)^2 n_{Ns}] = 140$ ns

T is limited by high n_{Ns} !

E= 6.3 MHz corresponds to the strain

ε = +1.5%

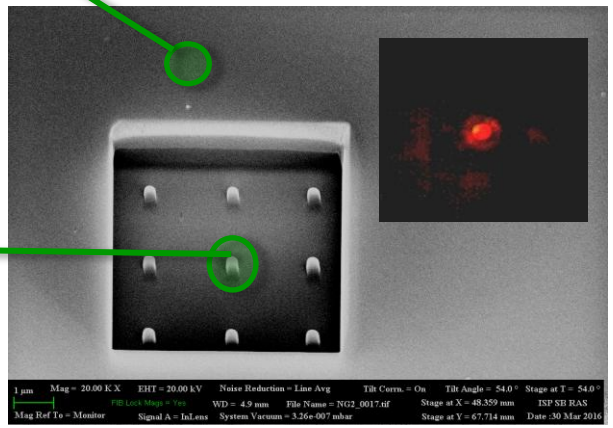

<NV's>
~50 pcs

Stimulated spin echo for T_2 measurements by MW pulse ODMR at constant laser excitation beam

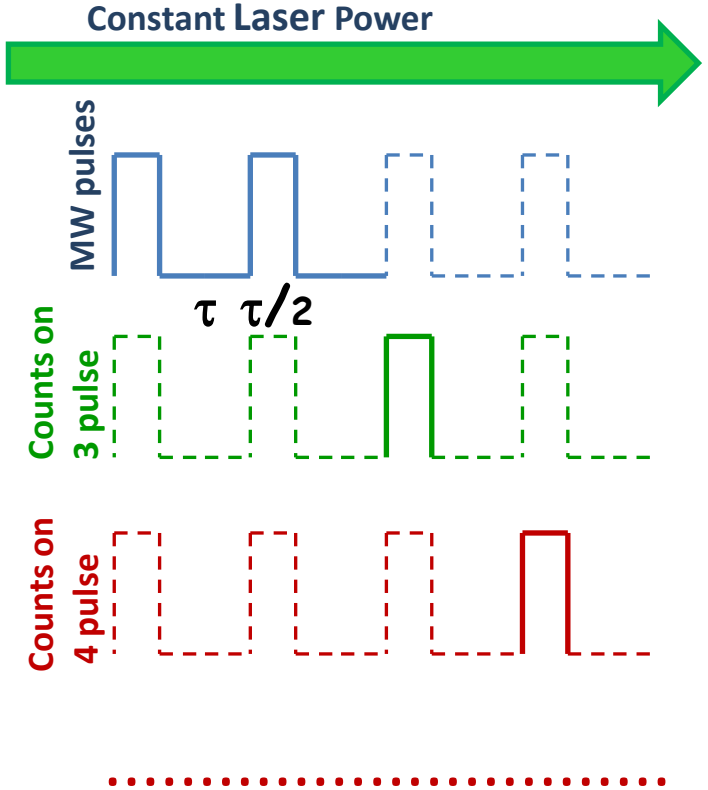

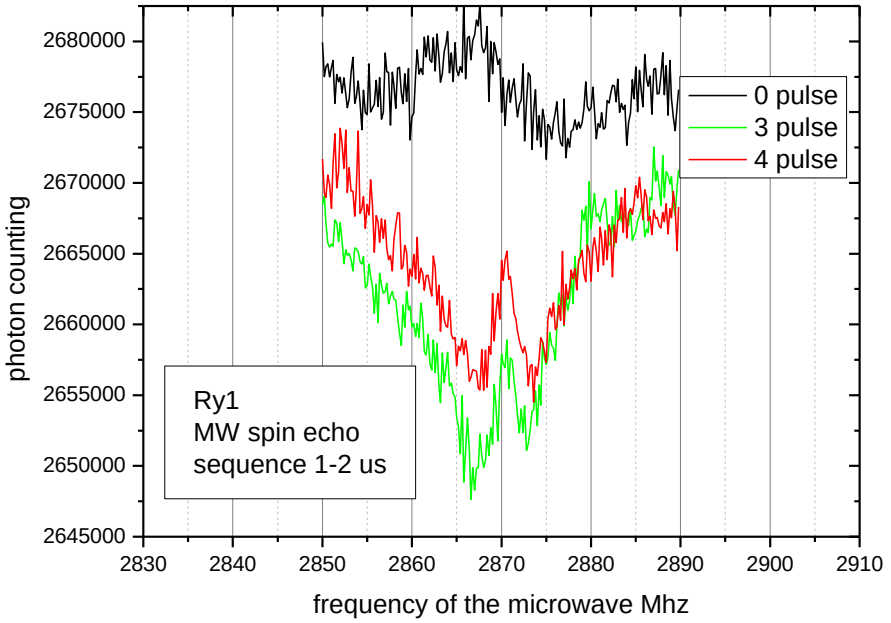

$$\frac{I3}{I4} = 1.3 = \exp\left(-\frac{2}{\tau} + \frac{5}{\tau}\right)$$

⇒ **30% decrease in ODMR dip after 5 μs means**

T_2 value ~ 12 μs

Conclusion

1. Hydrogen implantation with fluences $\Phi > 10^{17}$ cm^{-2} and HPHT annealing provide the buried conductive layer of mixed graphite forms with the resistivity < 10^{-3} Ohm·cm inside the diamond
2. Lift-off technique allows forming free and transferred membranes of diamonds as thin as 30 nm that are prospective for thin film vertical JFETs with a saturation current I_{on}= 50 mA/mm
3. The results for Schottki Barrier MISFET simulation using SB source-drain contacts show I_{on} as high as 100 mA/mm for optimized SB metals, or ~10 times higher than in normally-off MESFETs with H-transfer doping.
4. Hetero Barrier n-MISFET simulation with CN S-D regions shows the I_{on} as high as 100 mA/mm for optimized S-D doping or about ~100 times higher than in inversion channel n-MOSFETs but I_{on} depends strongly on effective mass of carriers under the barrier

Conclusion

1. Suspended diamond membranes as a gate of silicon FETs service as a highly sensitive sensors of displacements in the nanoscale range

2. NV-centers at the concentration 0.2-20 ppm in 30-300 nm layers and membranes have practically the same spectral characteristics as in the bulk diamond crystals

3. Charge state and ZPL position of NV-centers are effectively controlled by inner electric fields in p-n junction

4. NV center relaxation and spin coherence times are determined mainly by the interaction with nearest nitrogen donors and should be increased for QIP

5. NV matrices are the promising candidate for magnetic, electric, and spin nanoscopy and NMR spectroscopy with nanoscale resolution

Our thanks

to the colleagues from the Institutes of Semiconductor Physics, Geology and Mineralogy of SB RAS and Melbourne University :

Dr. L.N.Safronov for p-n & JFET fabrication,

Dr. A.A.Kalinin for HPHT treatment,

Dr. S. Rubanov for SEM analysis.

Thank Your for Attention!